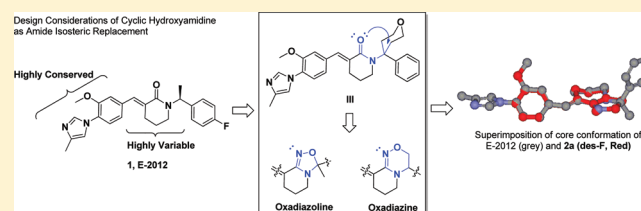


# Cyclic Hydroxyamidines as Amide Isoesters: Discovery of Oxadiazolines and Oxadiazines as Potent and Highly Efficacious $\gamma$ -Secretase Modulators in Vivo<sup>†</sup>

Zhong-Yue Sun,<sup>\*,‡</sup> Theodoros Asberom,<sup>‡</sup> Thomas Bara,<sup>‡</sup> Chad Bennett,<sup>‡</sup> Duane Burnett,<sup>‡</sup> Inhou Chu,<sup>#</sup> John Clader,<sup>‡</sup> Mary Cohen-Williams,<sup>§</sup> David Cole,<sup>‡</sup> Michael Czarniecki,<sup>‡</sup> James Durkin,<sup>‡</sup> Gioconda Gallo,<sup>‡</sup> William Greenlee,<sup>‡</sup> Hubert Josien,<sup>‡</sup> Xianhai Huang,<sup>‡</sup> Lynn Hyde,<sup>§</sup> Nicholas Jones,<sup>§</sup> Irina Kazakevich,<sup>‡</sup> Hongmei Li,<sup>‡</sup> Xiaoxiang Liu,<sup>‡</sup> Julie Lee,<sup>§</sup> Malcolm MacCoss,<sup>‡</sup> Mihir B. Mandal,<sup>‡</sup> Troy McCracken,<sup>‡</sup> Amin Nomeir,<sup>#</sup> Robert Mazzola,<sup>‡</sup> Anandan Palani,<sup>‡</sup> Eric M. Parker,<sup>§</sup> Dmitri A. Pissarnitski,<sup>‡</sup> Jun Qin,<sup>‡</sup> Lixin Song,<sup>§</sup> Giuseppe Terracina,<sup>§</sup> Monica Vicarel,<sup>‡</sup> Johannes Voigt,<sup>||</sup> Ruo Xu,<sup>‡</sup> Lili Zhang,<sup>§</sup> Qi Zhang,<sup>§</sup> Zhiqiang Zhao,<sup>‡</sup> Xiaohong Zhu,<sup>‡</sup> and Zhaoning Zhu<sup>\*,‡</sup>

<sup>‡</sup>Department of Medicinal Chemistry, <sup>§</sup>Department of Neuroscience, <sup>||</sup>Department of Structural Chemistry, <sup>†</sup>Department of Pharmaceutical Sciences, and <sup>#</sup>Department of Drug Metabolism and Pharmacokinetics, Schering Plough Research Institute, 2015 Galloping Hill Road, Kenilworth, New Jersey 07033, United States

**ABSTRACT:** Cyclic hydroxyamidines were designed and validated as isosteric replacements of the amide functionality. Compounds with these structural motifs were found to be metabolically stable and to possess highly desirable pharmacokinetic profiles. These designs were applied in the identification of  $\gamma$ -secretase modulators leading to highly efficacious agents for reduction of central nervous system  $A\beta_{42}$  in various animal models.



## INTRODUCTION

Alzheimer's disease (AD) is an ultimately fatal neurodegenerative disease that is the most common cause of age-related dementia. More than 35 million people suffer from AD worldwide, with an estimated annual cost of over \$600 billion, and the AD population may increase to more than 115 million by 2050 according to a report from Alzheimers Disease International.<sup>1</sup> A great collective effort is being made across academic and industrial laboratories to develop therapies to halt or even reverse AD. There are two distinct pathological hallmarks in the AD brains: extracellular amyloid plaques and intracellular neurofibrillary tangles. Amyloid plaques are composed of insoluble deposits of amyloid- $\beta$  ( $A\beta$ ), particularly  $A\beta_{42}$ , a 42 amino acid long peptide produced from its precursor protein (APP) through sequential cleavages by BACE1<sup>2</sup> and  $\gamma$ -secretase.<sup>3</sup>  $A\beta_{42}$  and its oligomers were found to be highly toxic in cells and were proposed<sup>4</sup> as the root cause for AD's pathology, leading to neurofibrillary tangle formation and eventual cell death.

$A\beta_{42}$ , despite being the predominant component of the amyloid plaque, is produced in minor proportion (5–10%) of the total  $A\beta$  species composed of  $A\beta_{37}$  to  $A\beta_{42}$ . They differ at the C-terminus because of poor selectivity at the  $\gamma$ -secretase cleavage step. Several classes of  $\gamma$ -secretase inhibitors (GSIs) have been reported to effectively eliminate production of all  $A\beta$  peptides in vitro and in vivo. However,  $\gamma$ -secretase has a wide variety of substrates in addition to APP that are involved in diverse biological processes. One of the most notable processes

is the Notch cleavage,<sup>5</sup> producing a cell surface receptor involved in regulating cell differentiation and proliferation.<sup>6</sup> GSI's selectivity issues against Notch and other biological pathways became a significant concern when their clinical trials identified higher incidence of skin cancer in the treatment group than in the placebo group among other known mechanism-based toxicological findings.<sup>7</sup>

In 2001, a class of small molecules was found that alter the product distribution among the known  $A\beta$  species without overall inhibition of the  $\gamma$ -secretase enzyme function including APP and Notch processing. GSMs selectively reduce certain  $A\beta$  species while enhancing the production of others.<sup>8,9</sup> A subclass of these  $\gamma$ -secretase modulators (GSMs) exemplified by some nonsteroidal anti-inflammatory drugs (NSAIDs) such as ibuprofen, indomethacin, and sulindac sulfide was found to elevate the level of the shorter  $A\beta$  species ( $A\beta_{37}$ ,  $A\beta_{38}$ , and  $A\beta_{39}$ ) while inhibiting longer and more toxic  $A\beta_{40}$  and  $A\beta_{42}$ . This type of GSM presents a unique approach to address the central tenet of the amyloid hypothesis (i.e.,  $A\beta_{42}$  inhibition) while effecting a gentler perturbation of  $A\beta$  natural metabolism, potentially leading to less mechanism-based toxicity involving  $A\beta$  and  $\gamma$ -secretase inhibition.<sup>10</sup> Therefore, it is highly attractive to identify GSMs that can selectively reduce  $A\beta_{42}$  and elevate the  $A\beta_{40}/A\beta_{42}$  ratio and can be evaluated as anti-AD agents for

Received: October 18, 2011

Published: November 18, 2011

their safety and efficacy profiles in comparison to other approaches targeting the  $A\beta$  process. Flurizan (Figure 1), the

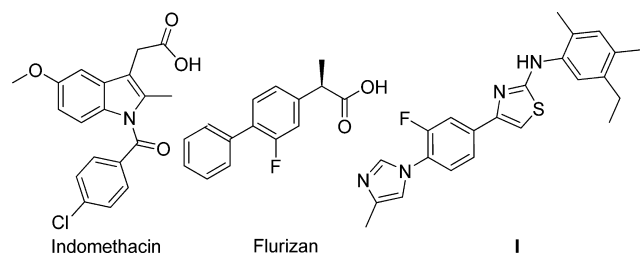


**Figure 1.** NSAID and non-NSAID  $\gamma$ -secretase modulators.

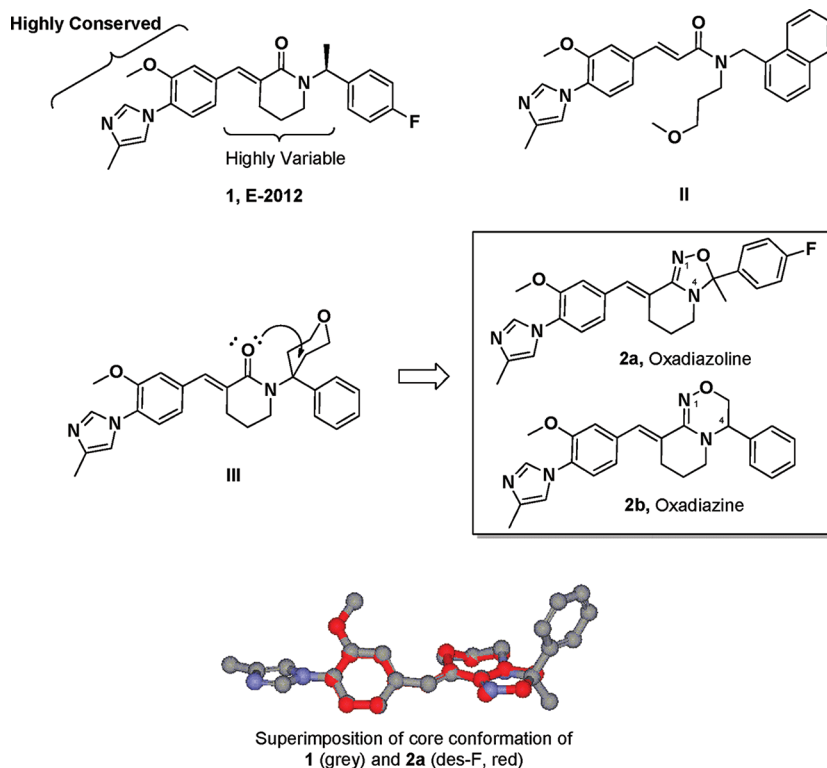
most advanced GSM developed by Myriad Genetics, failed to demonstrate statistically significant efficacy in AD patients in a phase III clinical trial. This result was not surprising given the compound's weak in vitro activity against  $\gamma$ -secretase  $A\beta_{42}$  cleavage and its poor central nervous system (CNS) penetration,<sup>11</sup> highlighting the need for a more potent and brain penetrant GSM.

In 2004, a new class of non-NSAID class of GSMs was reported by scientists from Torrey Pines Therapeutics<sup>12</sup> with impressive potency in reduction of  $A\beta_{42}$  in cells. Compound I (Figure 1) was also shown to reduce both plasma and brain  $A\beta_{42}$  and  $A\beta_{40}$  in Tg 2576 mice. Furthermore, chronic treatment of Tg 2576 mice with I lowered plaque density and amyloid load in both hippocampus and cortex.<sup>9</sup> Following this lead, a biaryl cinnamide class of GSM was reported later that preserved the imidazolylphenyl group with the central aminothiazole of I replaced by an  $\alpha,\beta$ -unsaturated amide (e.g., I, II, and III in Figure 2).<sup>13,14</sup> Compound I entered phase I clinical studies in 2006, but the clinical development was temporarily halted because of the finding of rat lenticular toxicity after administration of high doses for 13 weeks.<sup>8c</sup> In our

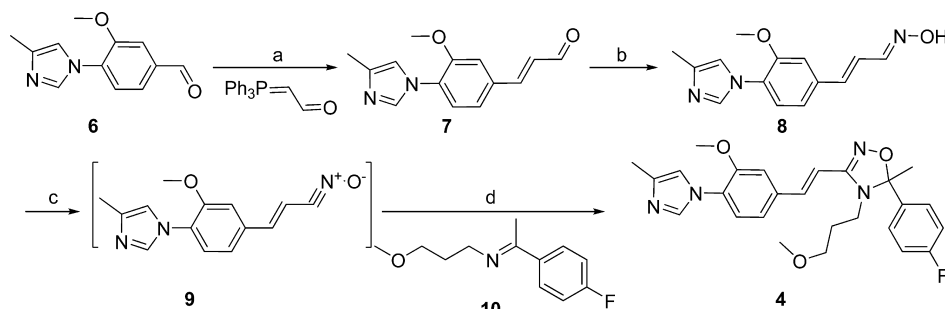
hands, E-2012 showed good in vitro potency (HEK 293<sup>Swe-Lon</sup> cell  $A\beta_{42}$   $IC_{50}$  = 64 nM) and a desirable GSM profile ( $A\beta_{total}/A\beta_{42}$   $IC_{50}$  ratio of 226). It also exhibits robust rat in vivo efficacy in reducing cerebrospinal fluid (CSF)  $A\beta_{42}$  by 55% and cortical  $A\beta_{42}$  by 44% after a single oral dose of 30 mg/kg.

## MODULATOR DESIGN

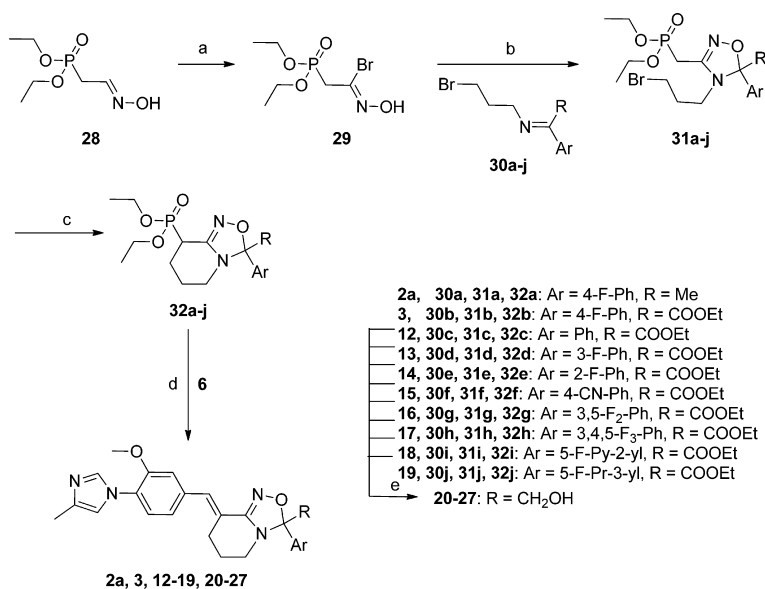
In an effort to design novel GSMs, we decided to focus on the non-NSAID GSM class represented by compound I and try to further optimize its overall profile and address its lenticular toxicity issue. A survey of related patent literature indicated that the imidazolylphenyl group is a highly conserved pharmacophore across multiple subclasses of modulators from a number of research laboratories. In contrast, the middle part of the molecule, represented by the  $\delta$ -lactam in I, can be highly variant, leaving room for exploration of a diverse range of structures. Realizing that compound I is a GSM with a highly optimized pharmacokinetic and pharmacodynamic profile, in our modulator design, we aimed to learn from its electronic topology while exploring significantly different chemical structures. One striking SAR point represented by the potent E-2012 analogue compound III ( $A\beta_{42}$   $IC_{50}$  = 56 nM, compound 639 in ref 13) indicates high tolerance in the enzyme environment around the quarternated benzylic position for large structural changes on this portion of the molecule. More importantly, the steric bulkiness at this site precluded the right-hand lone electron pair of the lactam carbonyl group from interacting with any potential H-bonding donor of the enzyme. The combination of potentially high tolerance for structural change and an idling right-hand lone electron pair on the carbonyl offers an attractive opportunity to build a ring from the position of the carbonyl oxygen to the benzylic position. An imino group would be required to offer an extra valence to form the ring while still preserving the left-hand lone pair electron



**Figure 2.** Design of 1,2,4-oxadiazoline as an amide isostere.

Scheme 1. Synthesis of Monocyclic Oxadiazoline 4<sup>a</sup>

<sup>a</sup>Reagents and conditions: (a) microwave 150 °C, 30 min, THF; (b) NH<sub>2</sub>OH·HCl, KOAc, MeOH; (c) NCS/Py, DCM; (d) Et<sub>3</sub>N, DCM.

Scheme 2. Synthesis of 5-Alkyl-5-aryl Bicyclic Oxadiazolines<sup>a</sup>

<sup>a</sup>Reagents and conditions: (a) NBS, DMF; (b) Et<sub>3</sub>N, DMF; (c) *t*-BuOK, THF; (d) *t*-BuOK, THF; (e) NaBH<sub>4</sub>, THF/MeOH.

density as a replacement of the carbonyl group. However, an imino group seldom is a viable replacement for the carbonyl because of its high basicity and reactivity; a neutral version of the imino group therefore should be a far better choice. Hydroxylated imines such as oximes, hydroxyamidines,<sup>15</sup> and hydroxyguanidines<sup>16</sup> are known to be much less basic than their imine counterparts and in most cases far more stable. Therefore, a cyclized oxadiazoline or oxadiazine appeared to be a reasonable isosteric replacement of the lactam carbonyl in **1**.

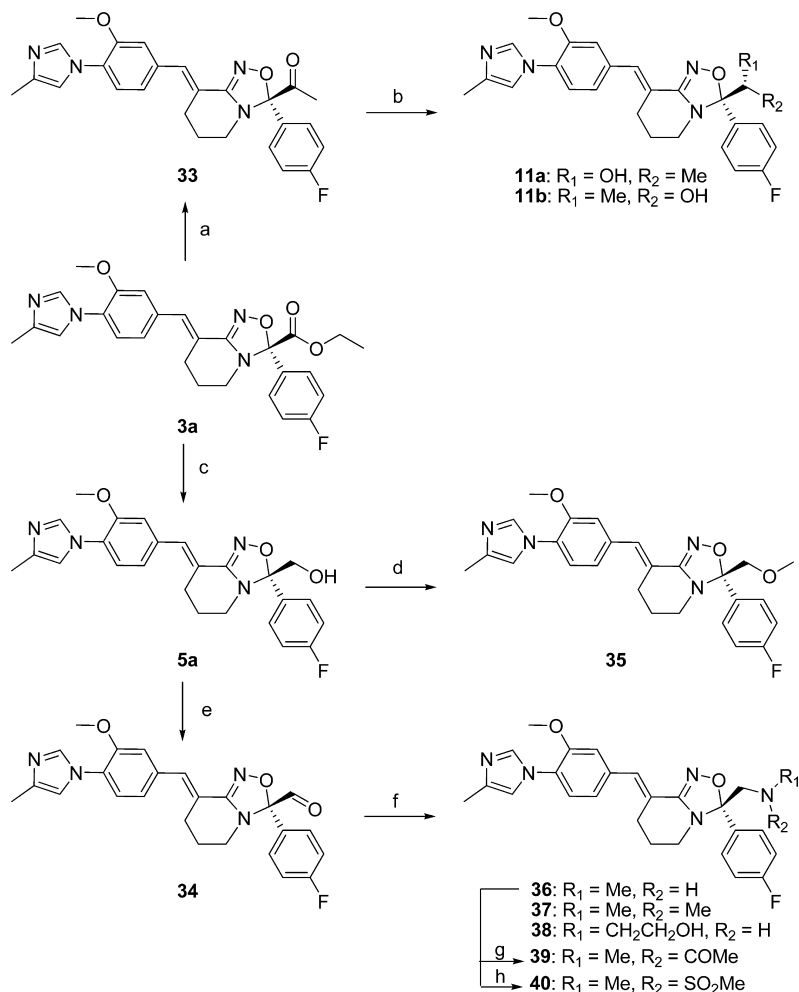
Comparing the core conformations of compound **1** (gray) and oxadiazoline **2a** (red), we found that they are completely superimposable (Figure 2). Molecular designs such as **2a** have minimum perturbation of electronic topology compared to **1** while offering a different molecular framework for us to further optimize its profile. However, oxadiazolines have not been explored as viable pharmacophores, and their metabolic and toxicological profiles were unknown. The monocyclic oxadiazolines seem unstable under acidic conditions,<sup>17</sup> but some fused tricyclic oxadiazolines are stable in hot 20% HCl in MeOH.<sup>18</sup> On the other hand, a ring expanded analogue of oxadiazoline, oxadiazine, has been explored in the context of p38 MAP kinase inhibitors, one of which was evaluated in phase II human clinic trials for cardiovascular disease.<sup>19</sup> In order to expeditiously

validate the proposal of isosteric replacement of the lactam carbonyl group with cyclic hydroxyamidines, we first focused on monocyclic oxadiazolines because of their straightforward syntheses. Despite their known stability issues, the monocyclic oxadiazolines (e.g., **4** in Scheme 1) should be a suitable probe for the validity of the GSM molecular design using the *in vitro* cellular assay, before more resource was applied to this direction. If successful, we planned to move to bicyclic oxadiazolines (e.g., **2a** in Figure 2) and oxadiazines (e.g., **2b** in Figure 2) to address any druggability issues.

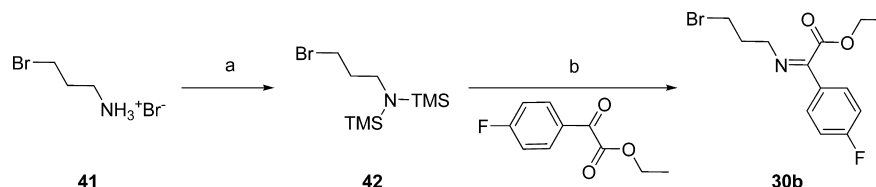
## CHEMISTRY

The monocyclic 1,2,4-oxadiazoline **4** was synthesized in three steps as outlined in Scheme 1. The imidazolylbenzaldehyde **6**<sup>13</sup> reacted with (formylmethylene)triphenylphosphorane to form imidazolylcinnamaldehyde **7** which was subsequently converted to oxime **8**. Nitrile oxide **9**, generated *in situ* by treatment of **8** with *N*-chlorosuccinimide and pyridine,<sup>20</sup> reacted with the ketimine **10** through a [3 + 2] dipolar cycloaddition to form compound **4**.

The bicyclic oxadiazoline compounds **2a**, **3**, and **12–19** were prepared as described in Scheme 2 from the key intermediate oxadiazolines (**31a–j**), which were synthesized from the [3 + 2]

Scheme 3. Synthesis of 3-(4-Fluorophenyl)-3-hydroxymethyl or 3-Aminomethyl Analogues<sup>a</sup>

<sup>a</sup>Reagents and conditions: (a) MeMgBr, Et<sub>3</sub>N, THF; (b) (*S*)-2-methyl-CBS-oxazaborolidine in toluene, BH<sub>3</sub>·Me<sub>2</sub>S, THF; (c) NaBH<sub>4</sub>, THF/MeOH; (d) MeI, NaH, DMF; (e) Swern oxidation. (f) For **36** and **37**: NaBH(OAc)<sub>3</sub>, HOAc, the corresponding amine, DCE. For **38**: the reductive amination with 2-aminoethylbenzoate followed by hydrolysis with LiOH. (g) Acetic anhydride, Et<sub>3</sub>N, DCM; (h) MeSO<sub>2</sub>Cl, Et<sub>3</sub>N, DCM.

Scheme 4. Synthesis of the Ketimine **30b**<sup>a</sup>

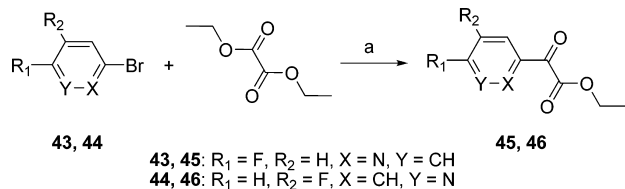
<sup>a</sup>Reagents and conditions: (a) TMSCl, Et<sub>3</sub>N, DCM; (b) TMSOTf, DCM, reflux.

dipolar cycloaddition of the corresponding 3-bromopropylketimines **30a–j** and a nitrile oxide generated from bromooxime **29** in situ.<sup>21</sup> A potassium *tert*-butoxide mediated cyclization of **31a–j** led to formation of the bicyclic oxadiazoline compounds **32a–j**, which were finally coupled with the imidazolylbenzaldehyde **6** using Horner–Emmons conditions to give **2a**, **3**, and **12–19**, respectively (Scheme 2).

The ester group in the bicyclic oxadiazolines **3** and **12–19** is highly versatile in order to access alcohols and other functional groups (Schemes 2 and 3). The success of the [3 + 2] cycloaddition was highly dependent on the quality of the corresponding imines, for which three synthetic methods had to be developed based on different starting amines and

ketones. Nonfunctionalized ketimine **10** was generated from 3-methoxypropylamine and 4-fluoroacetophenone using 3 Å molecular sieves as the dehydrating agent. Ketimine **30a** containing a 3-bromopropyl group was obtained with condensation conditions involving TiCl<sub>4</sub> and Et<sub>3</sub>N.<sup>22</sup> Formation of ketimines (**30b–j**) containing both ester and 3-bromopropyl groups was found to be most efficient using TMS triflate catalyzed imine synthesis from the TMS protected amine (**42**)<sup>23</sup> and the corresponding arylketoesters (Scheme 4)<sup>24</sup> that were obtained from the corresponding aryl bromides (**43**, **44**) and diethyl oxalate through the Grignard reaction as shown in Scheme 5.

Compound **3a** is an enantiomer obtained by resolving the racemate **3**. The absolute structure of **3a** was determined as the

Scheme 5. Synthesis of the Ketoesters 45 and 46<sup>a</sup>

<sup>a</sup>Reagents and conditions: (a) *i*-PrMgCl·LiCl, THF.

S-configuration through its hydroxyethyl derivatives **11a** and **11b**, using the NMR spectra of their corresponding Mosher's esters.<sup>25</sup>

As illustrated in Scheme 6, oxadiazine **53** was synthesized via lactam **51** which was prepared from **48** and **49** using a similar method described in ref 13. The enantiomer of amino alcohol **48** was synthesized by the Sharpless aminohydroxylation<sup>26</sup> from styrene **47**. By use of a Mitsunobu reaction/deprotection sequence, lactam **51** was then converted into hydroxylamine **52**, followed by cyclization using P<sub>2</sub>O<sub>5</sub> in refluxing EtOH overnight to yield oxadiazine **53** in 90% enantiomeric excess.

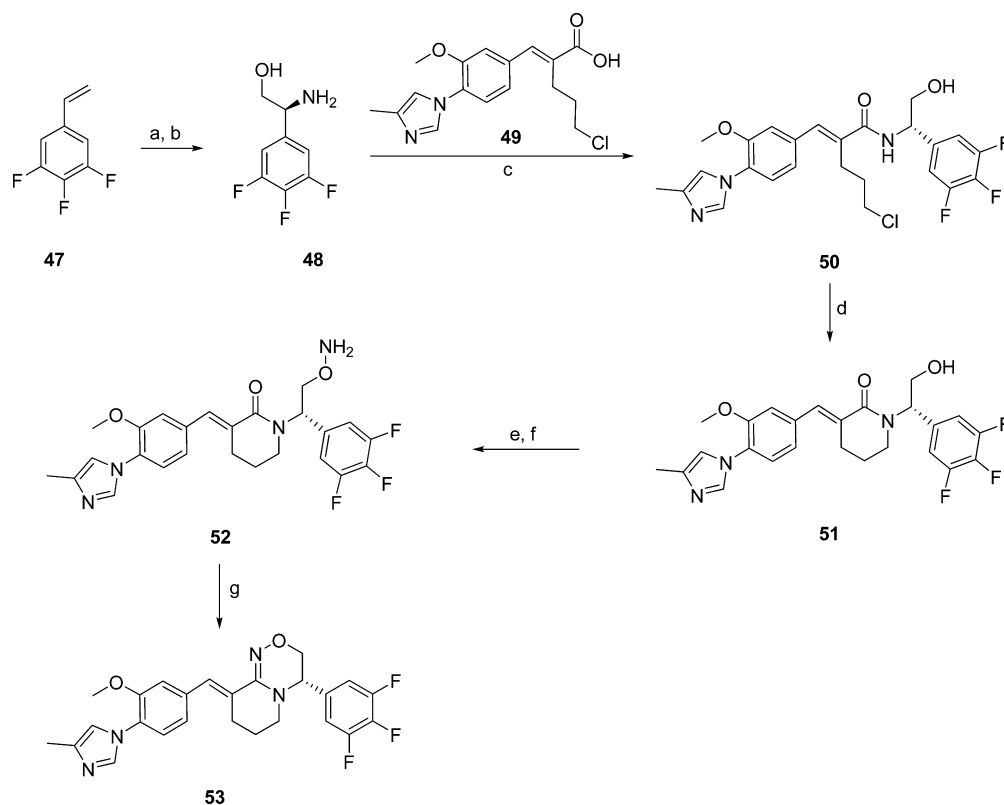
## RESULTS AND DISCUSSION

Racemic oxadiazoline **4**, designed based on compound **II** (Figure 2) for the initial GSM design validation, has IC<sub>50</sub> of 187 nM for Aβ<sub>42</sub> and IC<sub>50</sub> of 2 μM for Aβ<sub>40</sub> in the cellular assays. Compared to the IC<sub>50</sub> of compound **II** of 60 nM for Aβ<sub>42</sub> reduction, these data confirm the modulator profile and the validity of oxadiazoline as an isosteric replacement of the lactam carbonyl group. Compound **4** is stable under neutral conditions,

only slowly decomposing in aqueous 0.1 N HCl at room temperature over 3 h, leading to the corresponding acetophenone.

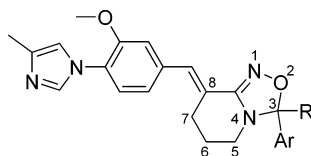
A cyclized version of the oxadiazoline such as compound **2a** would further stabilize the heterocyclic ring<sup>18</sup> and may lead to a suitable "druggable motif".<sup>27</sup> Indeed, the active enantiomer of racemic **2a(α)** is far more stable under the same conditions, with deterioration of enantiomeric excess from 99.6% to 55.7% overnight as the only observable change. The compound has a pK<sub>a</sub> of 6.7, a value higher than the reported pK<sub>a</sub> for 1-phenylimidazole (pK<sub>a</sub> = 5.1),<sup>28</sup> indicating that the oxadiazoline core is more basic than the *N*-phenylimidazole group. Compound **2a(α)** possesses an excellent pharmacokinetic profile in all animal species examined (Table 4) and has a low drug–drug interaction liability as evidenced by lack of inhibition of human cytochrome P450s, such as 3A4, 2D6, and 2C9, and lack of induction of human hPXR. It has a hERG ion channel IC<sub>50</sub> of 740 nM (Table 3) in a voltage clamp cellular assay and thus has some risk of QTc prolongation in humans. More interestingly, compound **2a(α)** demonstrates a pharmacological profile indistinguishable from E-2012 in vitro, with an IC<sub>50</sub> of 58 nM for reduction of Aβ<sub>42</sub> and an Aβ<sub>total</sub>/Aβ<sub>42</sub> IC<sub>50</sub> ratio of 237 in an HEK293 cell assay (Table 1). When administered to rats, compound **2a(α)** dose dependently reduces CSF levels of Aβ<sub>42</sub> by 51% and 30% 3 h after single oral doses of 10 and 3 mg/kg, respectively, with corresponding brain exposure of 5 and 0.8 μM.

The highly desirable in vitro and in vivo profile of **2a(α)** highlighted the urgency to resolve the hERG issue. A comprehensive medicinal chemistry effort was therefore launched to further optimize this series. Among many directions, we examined substitution effects on both 3-phenyl and 3-methyl

Scheme 6. Synthesis of Oxadiazine 53<sup>a</sup>

<sup>a</sup>Reagents and conditions: (a) CbzNH<sub>2</sub>, NaOH/*tert*-butyl hypochlorite, (DHQ)<sub>2</sub>PHAL, K<sub>2</sub>O<sub>8</sub>O<sub>2</sub>(OH)<sub>4</sub>, PrOH/water; (b) H<sub>2</sub>/Pd(OH)<sub>2</sub>; (c) EDCl, HOBT, DIEA, DMF; (d), NaOMe, MeOH; (e) *N*-hydroxyphthalimide, PPh<sub>3</sub>, DIAD, THF; (f) NH<sub>2</sub>NH<sub>2</sub>, EtOH; (g) P<sub>2</sub>O<sub>5</sub>, EtOH, reflux.

Table 1. In Vitro Activity of 3-Aryl-3-alkyl Substituted Bicyclic Oxadiazoline Analogues



compd	Ar	R	C3 config	IC <sub>50</sub> <sup>a</sup> nM		
				Aβ <sub>42</sub>	Aβ <sub>total</sub>	IC <sub>50</sub> (Aβ <sub>total</sub> )/IC <sub>50</sub> (Aβ <sub>42</sub> )
2a(α)	4-F-Ph	Me	<sup>b</sup>	58	13702	237
5a	4-F-Ph	CH <sub>2</sub> OH	S	29	14130	488
5b	4-F-Ph	CH <sub>2</sub> OH	R	7643	>20000	>3
20a	Ph	CH <sub>2</sub> OH	<sup>b</sup>	96	3210	33
21a	3-F-Ph	CH <sub>2</sub> OH	<sup>b</sup>	26	7164	280
22a	2-F-Ph	CH <sub>2</sub> OH	<sup>b</sup>	53	10052	189
23a	4-CN-Ph	CH <sub>2</sub> OH	<sup>b</sup>	117	>20000	>171
24a	3,5-di-F-Ph	CH <sub>2</sub> OH	<sup>b</sup>	21	6750	316
25a	3,4,5-tri-F-Ph	CH <sub>2</sub> OH	<sup>b</sup>	15	15810	1023
26a	5-F-Py-2-yl	CH <sub>2</sub> OH	<sup>b</sup>	103	19716	192
27a	5-F-Py-3-yl	CH <sub>2</sub> OH	<sup>b</sup>	106	>20000	>189

<sup>a</sup>Determined in HEK<sup>Swe-Lon</sup> 293 cells. <sup>b</sup>Active enantiomer.

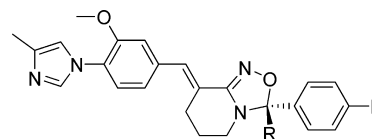
groups on the oxadiazoline ring as shown in Table 1 with an emphasis on reduction of hydrophobicity of these compounds (see also ref 14 for examples of similar approaches around E-2012). Hydroxylation of the 3-methyl group is tolerated with an eudismic ratio between the two enantiomers (**5a** and **5b**) higher than 260-fold. The *S*-configuration (**5a**) is the preferred stereochemistry, which agrees with what was reported for **1**. Additional fluorine substitution modestly improves potency with the 3,4,5-trifluorophenyl (**25a**) being the most potent (Aβ<sub>42</sub> IC<sub>50</sub> of 15 nM). Polar group incorporation into the 3-aryl group (**23a**, **26a**, and **27a**) had a negative impact on GSM potency.

Compound **5b**, with a pK<sub>a</sub> of 5.8, was found to be more stable compared to **2a(α)**, as it showed no sign of decomposition or deterioration of enantiomeric excess after 7 days at room temperature in 0.1 N HCl/MeOH (1:1). The excellent stability of **5b** can be attributed to the increased barrier to decomposition imposed by the inductive effect of 3-hydroxymethyl and potential stabilization from an intramolecular hydrogen bond between the hydroxyl group and the oxadiazoline oxygen.

Encouraged by the tolerance to the C3-methyl modification, we further explored the scope of the SAR at this position. Replacement of the C3-methyl group with either configuration of 1-hydroxyethyl is tolerated though no improvement was seen (**11a**, **11b**). Charged groups (**36**, **37**) seem to reduce modulator potency while the less basic hydroxyethylamino group has the least impact (**38**). Small nonbasic nitrogen derivatives such as amide (**39**) and sulfonamide (**40**) are modestly tolerated (Table 2).

With the full validation of five-membered cyclic hydroxyamides as lactam carbonyl isosteric replacement, we further explored other variations of this concept by first examining oxadiazines with a choice of trifluorophenyl group as exemplified by compound **53**. Compound **53** displays two pK<sub>a</sub> values of 7.4 and 2.7, indicating that the oxadiazine ring is modestly more basic than oxadiazolines. This weak basicity gives **53** a highly desirable aqueous solubility of greater than 100 mM at pH 3.5 as an HCl salt, despite the fact that its measured log *D* (5.29 at pH 7.4) suggested a molecule with a rather hydrophobic

Table 2. In Vitro Activity of (S)-3-(4-Fluorophenyl)-3-alkyl Substituted Bicyclic Oxadiazoline Analogues



compd	R	IC <sub>50</sub> <sup>a</sup> nM		IC <sub>50</sub> (Aβ <sub>total</sub> )/IC <sub>50</sub> (Aβ <sub>42</sub> )
		Aβ <sub>42</sub>	Aβ <sub>total</sub>	
11a	CH(OH)Me (R)	46	16237	350
11b	CH(OH)Me (S)	89	>20000	>225
35	CH <sub>2</sub> OMe	122	17466	144
36	CH <sub>2</sub> NHMe	191	>20000	>105
37	CH <sub>2</sub> NMe <sub>2</sub>	196	18833	96
38	CH <sub>2</sub> NHCH <sub>2</sub> CH <sub>2</sub> OH	80	>20000	>250
39	CH <sub>2</sub> N(Me)COMe	199	>20000	>101
40	CH <sub>2</sub> N(Me)SO <sub>2</sub> Me	72	19308	269

<sup>a</sup>Determined in HEK<sup>Swe-Lon</sup> 293 cells.

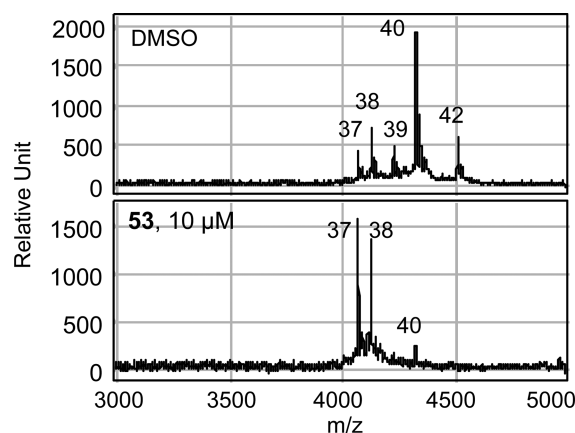
nature. Its nominal basicity notwithstanding, compound **53** is a very potent GSM in vitro, indicating an excellent isosteric replacement of the carbonyl group (Table 3).

Table 3. In Vitro Profiles of 2a(α), 5a, and 53

	2a(α)	5a	53	1
Aβ <sub>42</sub> IC <sub>50</sub> (nM) <sup>a</sup>	58	29	33	64
Aβ <sub>40</sub> IC <sub>50</sub> (nM) <sup>a</sup>	267	170	123	2300
Aβ <sub>total</sub> IC <sub>50</sub> (nM) <sup>a</sup>	14000	14130	>20000	14000
Notch IC <sub>50</sub> (nM) <sup>a</sup>		>50000	>50000	
hERG IC <sub>50</sub> (nM) <sup>b</sup>	740	3300	1000	1200
P <sub>a-b</sub> <sup>c</sup> (nm/s)	346	302	246	579
P <sub>b-a</sub> /P <sub>a-b</sub> <sup>c</sup>	0.6	1.4	2	1.2

<sup>a</sup>determined in HEK293<sup>Swe-Lon</sup> cells. <sup>b</sup>determined using a voltage-clamp method. <sup>c</sup>P<sub>a-b</sub> is the permeability when applied to the apical side, while P<sub>b-a</sub> is the permeability when applied to the basolateral side in a Caco-2 membrane assay (nm/s). The ratio of these two values is a measure of Pgp efflux, while the P<sub>a-b</sub> value is a measure of permeability.

The GSM characteristics of **5a** and **53** were further confirmed by the changes they induce in the  $A\beta$  species produced by HEK293<sup>Swe-Lon</sup> cells in vitro as assessed by mass spectrometry. Incubation of HEK293<sup>Swe-Lon</sup> with 10  $\mu$ M **53** selectively reduced  $A\beta_{42}$ ,  $A\beta_{40}$ , and  $A\beta_{39}$  while profoundly increasing production of  $A\beta_{37}$  and  $A\beta_{38}$  (Figure 3). A similar modulator profile was also observed for **5a**.



**Figure 3.** Mass spectrometric analysis of  $A\beta$  peptides generated from HEK293<sup>Swe-Lon</sup> cells after treatment with vehicle (DMSO) or 10  $\mu$ M **53**.

Compounds **5a** and **53** are highly permeable in a Caco-2 membrane permeability assay and do not appear to be substrates for PGP efflux (Table 3).<sup>29</sup> These two compounds possess excellent pharmacokinetic profiles typical of their structural classes in dog, rat, and monkey (Table 4). Both compounds displayed a better overall hERG profile than compound **2a**( $\alpha$ ) because both reduced potency for blocking the hERG channel and decreased exposure at the effective doses (Table 3). Neither compound affected QTc intervals in dogs at sufficient exposure multiples over exposures required for pharmacological effect (data not shown).

Compounds **5a** and **53** did not inhibit APP processing (Table 3) in vitro as indicated by a lack of substrate accumulation of C89 and C100, the cleavage products of preceding  $\alpha$ -secretase and BACE1 cleavages. Nor did they affect Notch processing in HEK293 cells expressing the human Notch1 protein at concentrations up to 50  $\mu$ M. The shift in specificity of APP cleavage (Figure 3) rather than a reduction in overall  $\gamma$ -secretase activity and the resulting lack of changes in substrate accumulation and Notch processing confirm that both compounds are potent GSMs. There was no evidence of Notch-related

side effects or biomarker changes following repeated administration of the highest tolerable doses of **5a** and **53** to rats. Neither compound produced goblet cell meta/hyperplasia in the ileum, nor did they decrease thymus size or dramatically affect body weight, all of which are common side effects of  $\gamma$ -secretase inhibitors that reduce Notch cleavage. In addition, HES-1 and adipsin expression, biomarkers for Notch activity, were unaffected in the jejunum of treated rats.

Compound **53** (3 mg/kg, orally) reduces cortical  $A\beta_{42}$  to 63% of the level seen after vehicle administration, while **5a** (10 mg/kg, orally) reduces cortical  $A\beta_{42}$  levels to 37% (Table 5). Compounds **5a** and **53** were also found to dose-dependently reduce  $A\beta_{42}$  preferentially over  $A\beta_{\text{total}}$  and  $A\beta_{40}$  upon acute administration to rat (Figure 4). Similar results were observed after sub-chronic (6 day) dosing in rat (data not shown). Four hours after a single dose of 30 mg/kg to cynomolgous monkeys ( $n = 3$ ), **53** reduces  $A\beta_{42}$  in the cortex and CSF to 44% and 70% of the values seen after vehicle administration (Figure 5). The corresponding plasma exposure of **53** 4 h after administration to the monkeys was  $\sim 6 \mu$ M, while the average brain/plasma ratio in the monkeys was determined to be 1.4.

## SUMMARY AND CONCLUSION

Cyclic hydroxyamidines were designed as novel isosteric replacements of amide with a consideration of hydrogen bonding characteristics and lack of strong basicity. Both five-membered oxadiazolines and six-membered oxadiazines were found to be ideal replacements for a lactam group. Importantly, these novel druggable motifs were found to possess highly desirable pharmacokinetic and toxicological profiles, offering excellent opportunities for exploration of amide bond replacement, a frequently encountered but potentially difficult task in drug discovery. Most valuable of all, both scaffolds were found to be modestly basic, enabling salt formation for rapid dissolution with an appropriate formulation while maintaining amide characteristics at physiological pH. The successful and expeditious validation of these novel amide isosteres led to GSMs that are highly efficacious in vitro and in vivo in a number of animal models. Further exploration of these compounds as potential drugs to fight Alzheimer's disease is underway and will be subjects of additional publications.

## EXPERIMENTAL SECTION

**Cell Based  $\gamma$ -Secretase Assay.** Human embryonic kidney (HEK) 293 cells stably transfected with a human APP cDNA with both the Swedish and London familial AD mutations in the pcDNA3.1 vector (Invitrogen, HEK293<sup>Swe-Lon</sup> cells) were treated with GSM

**Table 4.** PK Parameters in Rat, Dog, and Monkey<sup>a</sup>

compd	species <sup>a</sup>	AUC <sup>b</sup> ( $\mu$ M·h)	$C_{\text{max}}$ <sup>b</sup> ( $\mu$ M)	BA <sup>c</sup> (%)	$T_{1/2}$ <sup>d</sup> (h)	$V_{\text{dss}}$ <sup>d</sup> (L/kg)	CL <sup>d</sup> ( $\text{mL min}^{-1} \text{kg}^{-1}$ )
<b>2a</b> ( $\alpha$ )	rat	19	4.9	78	2.5	1.6	6.8
	dog	27	5.3	69	1.7	2.2	23
	monkey	30	5.6	57	2	1	7.3
<b>5a</b>	rat	61	7.5	98	3.4	1.6	6.1
	dog	26	4.0	38	1.4	0.4	5
	monkey	30	8.8	48	3	1.4	6
<b>53</b>	rat	265	19.8	100	3.5	0.4	1.4
	dog	27	7.9	69	0.8	0.6	9
	monkey	11	4.9	34	0.9	0.8	11

<sup>a</sup>10 mg/kg for po; 3 mg/kg for iv in rat, dog, and monkey. <sup>b</sup>AUC (area under the curve) and  $C_{\text{max}}$  (maximal drug concentration) obtained with po administration. <sup>c</sup>BA: bioavailability. <sup>d</sup> $T_{1/2}$  (half-life),  $V_{\text{dss}}$  (steady state volume of distribution), and CL (in vivo clearance) obtained with iv administration.

Table 5. In Vivo Profile of 5a and 53 in Rat

compd	po (mg/kg)	plasma ( $\mu\text{M}$ )	B/P ratio	CSF A $\beta$ (%) <sup>a</sup>			cortex A $\beta$ (%) <sup>a</sup>		plasma A $\beta$ (%) <sup>a</sup>		
				A $\beta_{42}$	A $\beta_{40}$	A $\beta_{\text{total}}$	A $\beta_{42}$	A $\beta_{40}$	A $\beta_{42}$	A $\beta_{40}$	A $\beta_{\text{total}}$
5a	10	3.6	0.15	66	104	120	37 <sup>b</sup>	77	41 <sup>b</sup>	44 <sup>b</sup>	77
53 <sup>c</sup>	3	3	0.49	65	74	88	63	84	32	50	86

<sup>a</sup>Expressed as % vehicle in CSF, cortex, and plasma at 3 h after dosing. <sup>b</sup> $p < 0.05$  vs vehicle-treated rats (ANOVA on raw values followed by Dunnett's post hoc  $t$  test comparing each treatment group to vehicle). <sup>c</sup>Results for 53 are average of data from several studies; see Figure 4 for data and variance.

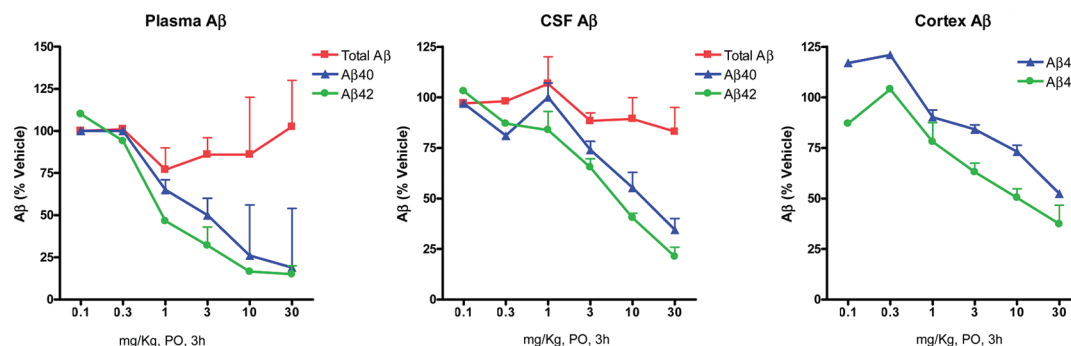


Figure 4. A $\beta_{\text{total}}$ , A $\beta_{40}$ , and A $\beta_{42}$  in plasma (left), CSF (middle), and cortex (right) from rats treated acutely with various single oral doses of 53 (1–30 mg/kg). Data are the mean  $\pm$  standard error of the mean averaged from several studies, expressed as % vehicle.

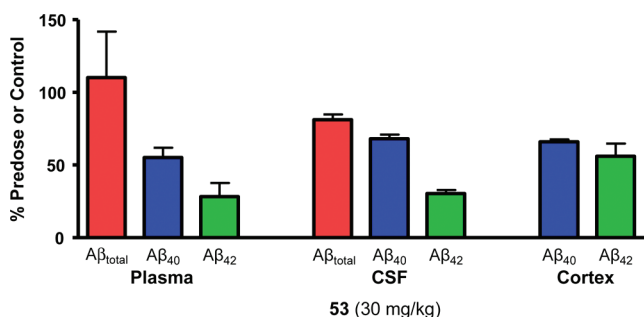


Figure 5. A $\beta_{\text{total}}$ , A $\beta_{40}$ , and A $\beta_{42}$  in plasma, CSF, and cortex from monkeys treated with 53 orally at 30 mg/kg at 4 h. Data are expressed as a percent of the predose value from the same animals (plasma) or as a percent of the control (vehicle)-treated monkeys (CSF and cortex).

compounds for 5 h. A $\beta$  in conditioned medium was measured using MesoScale Discovery (MSD) technology-based sandwich immunoassays. A $\beta_{42}$  was measured using a pair of labeled antibodies TAG-G2-11 and biotin-4G8. A $\beta_{40}$  was measured using the antibody pair of TAG-G2-10 and biotin-4G8; total A $\beta$  was measured using TAG-W02 and biotin-4G8. In some cases, a cell based  $\gamma$ -secretase assay was also carried out in HEK293 cells stably coexpressing a C99 expression construct and PS1 $\Delta\text{E9}$ , a familial Alzheimer's disease mutant form presenilin.<sup>30</sup> A $\beta$  in conditioned medium was measured using the same methods described above.

**Mass Spectrometric Analysis of A $\beta$  Profiles.** The A $\beta$  profile in conditioned medium was analyzed using surface enhanced laser desorption/ionization (SELDI) mass spectrometry as described previously.<sup>31</sup> The  $\gamma$ -secretase mixture of 50  $\mu\text{L}$  was applied on a PS20 protein chip array (BioRad) that had been precoated with 1  $\mu\text{g}$  of antibody W02. The array was incubated overnight at 4  $^{\circ}\text{C}$ . Nonspecific protein binding to the array was removed by washing three times in phosphate buffered saline (PBS) with 0.2% Tween 20 followed by three times in PBS. The array was rinsed briefly with water and air-dried before being analyzed on BioRad.

**Notch Assay.** HEK293 cells stably expressing a human Notch protein with a truncated extracellular EGF repeat domain (N $\Delta\text{E}$ )<sup>32</sup> were treated with GSI or GSM compounds. Production of the Notch intracellular domain (NICD) in cell lysates was measured using a

MSD-based sandwich immunoassay with Notch antibodies (Cell Signaling).

**CSF and Brain A $\beta$  Assays.** CSF A $\beta_{42}$  was measured using AlphaLISA A $\beta_{1-42}$  and A $\beta_{1-40}$  kits (Perkin-Elmer) according to the manufacturer's instructions. CSF total A $\beta$  was measured using MesoScale Discovery technology with biotinylated antibody 4G8 (Signet) and S-tag labeled antibody W02. A $\beta$  from rat and monkey brain was enriched by solid phase extraction using an Oasis HLB LP 96-well plate (Waters Corp.) and analyzed using AlphaLISA A $\beta_{1-42}$  and A $\beta_{1-40}$  kits.

**Drug Treatment in Animals.** Male CD rats ( $\sim 100$  g, Crl:CD-SD); Charles River Laboratories, Kingston, NY) were group housed and acclimated to the vivarium for 5–7 days prior to use in a study. Compounds were formulated in 20% hydroxypropyl- $\beta$ -cyclodextrin and administered orally with a dosing volume of 5 mL/kg. Three hours after drug administration, rats were euthanized with excess CO<sub>2</sub>. Immediately following euthanasia, CSF was collected from the cisterna magna and quickly frozen on dry ice. Only visibly clear CSF samples were analyzed. Blood was collected from the vena cava, and plasma was isolated using heparin as an anticoagulant. Finally, the brain was removed from the skull and immediately frozen on dry ice. All tissues were stored at  $-70$   $^{\circ}\text{C}$  until A $\beta$  quantification.

Adult male purpose bred cynomolgus monkeys (*Macaca fascicularis*), weighing between 6 and 8 kg, were used. Monkeys were fasted overnight prior to orogastric gavage tube administration of compound (formulated in 0.4% MC with 1–2 equiv of tartrate acid as an excipient) in a 1 mL/kg dosing volume. Three hours after drug administration, monkeys were given an intramuscular injection of ketamine HCl, a blood sample was collected from the femoral vein, and the animals were euthanized by an intravenous dose of sodium pentobarbital. CSF was collected from the cisterna magna immediately following euthanasia, and then the brain was removed and frozen on dry ice.

**Chemistry.** <sup>1</sup>H NMR spectra were measured on a Varian Oxford 400 or Bruker 500 UltraShield spectrometer. Chemical shifts  $\delta$  are reported relative to CDCl<sub>3</sub> at 7.26 ppm as an internal standard. LCMS spectra were obtained on a Shimadzu VP-Sciex API 150EX system. HPLC spectra were obtained on a Shimadzu VP system. Normal phase column chromatography was performed on prepacked silica gel columns using ISCO CombiFlash system. Reverse phase column chromatography was performed on Phenomenex Luna 10  $\mu\text{m}$  C18



columns using Alltech 627 HPLC pump or Varian SD-1 HPLC system. Chiral columns were from Chiral Technologies. The purity of final compounds was analyzed on two independent reverse phase HPLC systems with different gradient. LC–electrospray mass spectrometry with a C-18 column using a gradient of 5–95% MeCN in water as the mobile phase was used to determine the molecular mass and retention time. The purity of the samples was assessed using a mass detector and a UV detector at 254 nm. An additional analytical reverse phase HPLC system was used to assess the purity of final compounds using a UV detector monitored at both 219 and 254 nm and an ELSD detector. All compounds have purity greater than 95%.

**(E)-3-(4-Fluorophenyl)-8-(3-methoxy-4-(4-methyl-1H-imidazol-1-yl)benzylidene)-5,6,7,8-tetrahydro-3H-[1,2,4]-oxadiazolo[4,3-a]pyridine (2a) and Its Enantiomers (2a( $\alpha$ ) and 2a( $\beta$ )).** 2a, 2a( $\alpha$ ), and 2a( $\beta$ ) were prepared from 30a similar to the method for 3, 3a, and 3b. Compound 2a was resolved on an OD column, eluting with 50% isopropanol in hexanes containing 0.1% Et<sub>2</sub>NH to give 2a( $\alpha$ ) and 2a( $\beta$ ). <sup>1</sup>H NMR (400 MHz, CDCl<sub>3</sub>):  $\delta$  7.81 (1H, s), 7.58–7.55 (2H, m), 7.51 (1H, s), 7.26–7.24 (1H, d), 7.10–7.06 (2H, t), 7.02–7.00 (1H, d), 6.98 (1H, s), 6.94 (1H, s), 3.85 (3H, s), 3.17–3.12 (1H, m), 2.87–2.78 (1H, m), 2.78–2.69 (1H, m), 2.69–2.60 (1H, m), 2.32 (3H, s), 1.97–1.78 (2H, m), 1.89 (3H, s). LCMS for 2a( $\alpha$ ): *m/z* 433 [M + 1]<sup>+</sup>, 100% purity. LCMS for 2a( $\beta$ ): *m/z* 433 [M + 1]<sup>+</sup>, 99.9% purity.

**(E)-Ethyl 3-(4-Fluorophenyl)-8-(3-methoxy-4-(4-methyl-1H-imidazol-1-yl)benzylidene)-5,6,7,8-tetrahydro-3H-[1,2,4]-oxadiazolo[4,3-a]pyridine-3-carboxylate (3), and Its S-enantiomer (3a) and R-Enantiomer (3b).** Under N<sub>2</sub> protection, a solution of potassium *t*-BuOK (22.3 g, 199.5 mmol) in anhydrous THF (200 mL) was added slowly to a solution of 32b (81.3 g, 190.0 mmol) and 3-methoxy-4-(4-methyl-1H-imidazol-1-yl)benzaldehyde (6) (39.0 g, 180.5 mmol) in anhydrous THF (1900 mL) at –78 °C. The reaction mixture was stirred at –78 °C for 45 min, allowed to warm to –20 °C over a period of 30 min, diluted with brine, and extracted with EtOAc. The combined organic phase was washed with brine, dried over anhydrous Na<sub>2</sub>SO<sub>4</sub>, and concentrated under reduced pressure to give 3 (91 g, crude). This product (88 g) was resolved in an AS column, eluting with 55% isopropanol in hexanes containing 0.1% Et<sub>2</sub>NH to give the S-enantiomer 3a (30.6 g, 34.8% yield) and the R-enantiomer 3b. Analytical data for 3a: <sup>1</sup>H NMR (400 MHz, CDCl<sub>3</sub>)  $\delta$  7.70 (1H, s), 7.53–7.47 (3H, m), 7.24–7.22 (1H, d), 7.13–7.09 (2H, t), 7.00–6.98 (1H, d), 6.96 (1H, s), 6.91 (1H, s), 4.40–4.28 (2H, m), 3.83 (1H, s), 3.58–3.55 (1H, m), 2.88–2.85 (1H, m), 2.76–2.63 (2H, m), 2.28 (3, s), 1.99–1.91 (1H, m), 1.73–1.69 (1H, m), 1.35–1.31 (3H, t). LCMS *m/z* 491 [M + 1]<sup>+</sup>, 100% ee. 3b: LCMS *m/z* 491 [M + 1]<sup>+</sup>, 99% ee.

**(E)-5-(4-Fluorophenyl)-3-(3-methoxy-4-(4-methyl-1H-imidazol-1-yl)styryl)-4-(3-methoxypropyl)-5-methyl-4,5-dihydro-1,2,4-oxadiazole (4).** A mixture of 4-fluoroacetophenone (1.36 g, 9.9 mmol), 3-methoxypropylamine (1.76 g, 19.8 mmol), 3 Å molecular sieves, and 18 mL of DCM in a sealed tube was heated at 50 °C for 3 h and then was at room temperature for several days. The filtrate was concentrated under reduced pressure to give 10 (1.03 g). A mixture of 8 (100 mg, 0.39 mmol), NCS (51.9 mg, 0.39 mmol), and pyridine (7.8 mg, 0.1 mmol) in DCM (1.2 mL) was stirred at room temperature for 10 min, followed by additions of 10 (98 mg, 0.39 mmol) and Et<sub>3</sub>N (0.8 mL). The reaction mixture was stirred overnight, diluted with DCM, washed with water, and dried over anhydrous Na<sub>2</sub>SO<sub>4</sub>. The crude was purified on a silica gel column MeOH containing 2% Et<sub>3</sub>N/DCM with a gradient from 0% to 5%, followed by purification on a C18 column, eluting with MeCN/water containing 0.1% formic acid to give 4 (27 mg). <sup>1</sup>H NMR (400 MHz, CDCl<sub>3</sub>):  $\delta$  7.80 (1H, br s), 7.59–7.54 (2H, m), 7.48–7.44 (1H, d), 7.27–7.25 (1H, d), 7.18–7.16 (1H, d), 7.12 (1H, s), 7.08–7.04 (2H, t), 6.94 (1H, br s), 6.58–6.54 (1H, d). LCMS *m/z* 465 [M + 1]<sup>+</sup>, 97.7% purity.

**(S,E)-3-(4-Fluorophenyl)-8-(3-methoxy-4-(4-methyl-1H-imidazol-1-yl)benzylidene)-5,6,7,8-tetrahydro-3H-[1,2,4]-oxadiazolo[4,3-a]pyridin-3-yl)methanol (5a) and (R,E)-3-(4-Fluorophenyl)-8-(3-methoxy-4-(4-methyl-1H-imidazol-1-yl)benzylidene)-5,6,7,8-tetrahydro-3H-[1,2,4]oxadiazolo[4,3-a]pyridin-3-yl)methanol (5b).** Method a. Sodium borohydride (1.3 g, 34. mmol) was added to a solution of 3a (11.4 g, 23.2 mmol)

in anhydrous THF (116 mL) in an ice bath, followed by slow addition of anhydrous MeOH. The reaction mixture was stirred at room temperature for 2 h, quenched with a mixture of ice and brine, and extracted with EtOAc. The combined organic phase was washed with brine, dried over anhydrous Na<sub>2</sub>SO<sub>4</sub>, and concentrated under reduced pressure. The crude was purified on a silica gel column, eluting with MeCN containing 5% Et<sub>3</sub>N/EtOAc with a gradient from 0% to 100% to give 5a (8.1 g, 77.7% yield). <sup>1</sup>H NMR (400 MHz, CDCl<sub>3</sub>):  $\delta$  7.72 (1H, s), 7.52–7.48 (2H, m), 7.45 (1H, s), 7.26–7.23 (1H, d), 7.16–7.08 (2H, t), 7.03–6.96 (2H, m), 6.92 (1H, s), 4.23–4.19 (1H, d), 4.09–4.05 (1H, d), 3.84 (3H, m), 3.36–3.32 (1H, m), 2.99–2.75 (1H, m), 2.75–2.68 (2H, m), 2.60 (1H, br s), 2.29 (3H, s), 2.04–1.92 (1H, m), 1.92–1.80 (1H, m). LCMS *m/z* 449 [M + 1]<sup>+</sup>, 99.0% purity. Compound 5b was prepared from 3b by the same method. HPLC: 96.8% purity.

**Method b.** Compound 3 (3 g, crude) was reduced according to method a to give 5 (2.8 g, crude). This product (500 mg) was resolved on an AD column, eluting with 65% isopropanol in hexanes containing 0.1% Et<sub>2</sub>NH to give 5a (183 mg, 36.6%) and 5b.

**(E)-3-(3-Methoxy-4-(4-methyl-1H-imidazol-1-yl)phenyl)acrylaldehyde (7).** A solution of 3-methoxy-4-(4-methyl-1H-imidazol-1-yl)benzaldehyde (6) (1.00 g, 4.6 mmol) and (formylmethylene)triphenylphosphorane (1.83 g, 6.0 mmol) in THF was heated at 150 °C in a microwave reactor for 30 min. Solvent was evaporated under reduced pressure, and the residue was purified on a silica gel column, eluting with EtOAc/hexanes in a gradient from 0% to 100% to give 7 (1.05 g), which was used without further purification in the preparation of 8.

**3-(3-Methoxy-4-(4-methyl-1H-imidazol-1-yl)phenyl)acrylaldehyde Oxime (8).** Hydroxylamine hydrochloride (2.35 g, 33.8 mmol) was added portionwise to a solution of 7 (6.3 g, 26.0 mmol) and potassium acetate in MeOH (300 mL) in an ice bath. The reaction mixture was stirred at 0 °C for 90 min and then at room temperature for 30 min. Solvent was evaporated under reduced pressure. The residue was partitioned in EtOAc and brine, and aqueous NaHCO<sub>3</sub> was added to adjust the pH to 8. The aqueous phase was extracted with EtOAc, and the combined organic phase was washed with brine and dried over anhydrous Na<sub>2</sub>SO<sub>4</sub>. The crude was briefly purified on a C18 column, eluting with MeCN/water containing 0.02% concentrated HCl. The collected fraction was concentrated under reduced pressure to remove MeCN, neutralized with aqueous NaHCO<sub>3</sub>, and extracted with EtOAc to give 8 (2.48 g). LCMS *m/z* 258 [M + 1]<sup>+</sup>. It was used without further purification in the preparation of 4.

**(R)-1-((S,E)-3-(4-Fluorophenyl)-8-(3-methoxy-4-(4-methyl-1H-imidazol-1-yl)benzylidene)-5,6,7,8-tetrahydro-3H-[1,2,4]-oxadiazolo[4,3-a]pyridin-3-yl)ethanol (11a) and (S)-1-((S,E)-3-(4-Fluorophenyl)-8-(3-methoxy-4-(4-methyl-1H-imidazol-1-yl)benzylidene)-5,6,7,8-tetrahydro-3H-[1,2,4]oxadiazolo[4,3-a]pyridin-3-yl)ethanol (11b).** Under N<sub>2</sub> protection, a 1 M solution of (S)-2-methyl-CBS-oxazaborolidine (4.1 mL, 4.1 mmol) in toluene was added to a solution of the crude 33 (2.2 g, 4.9 mmol) in anhydrous THF (15 mL) at room temperature, followed by slow addition of 2 M solution of BH<sub>3</sub>·Me<sub>2</sub>S (3.7 mL, 7.3 mmol) in THF. The reaction solution was stirred for 2 h, quenched with a mixture of brine and ice, and extracted with EtOAc. The combined organic phase was washed with brine and dried over anhydrous Na<sub>2</sub>SO<sub>4</sub>. The crude was purified on a silica gel column, eluting with EtOAc/hexanes from 0% to 100%. The desired fraction was concentrated under reduced pressure. The resulting residue (1.3 g) was dissolved in THF (27 mL), treated with concentrated hydrochloride (0.45 mL, 5.5 mmol) at room temperature for 1 h, neutralized with aqueous NaHCO<sub>3</sub>, concentrated under reduced pressure, diluted with brine, and extracted with EtOAc. The combined organic phase was washed with brine and dried over anhydrous Na<sub>2</sub>SO<sub>4</sub>. The crude was purified on a C18 column, eluting with MeCN/water containing 0.1% TFA. The desired fractions were neutralized with aqueous NaHCO<sub>3</sub>, concentrated under reduced pressure, and extracted with EtOAc to give 11a (0.56 g, 25.3% yield) and 11b (0.12 g, 5.4% yield). Analytical data for 11a: <sup>1</sup>H NMR (400 MHz, CDCl<sub>3</sub>)  $\delta$  7.94 (1H, s), 7.50–7.46 (2H, m), 7.42 (1H, s), 7.23–7.21 (1H, d), 7.11–7.07 (2H, t), 6.97–6.91 (3H, m), 4.53–4.49 (1H, q), 3.82 (3H, s), 3.42–3.37 (1H, m), 2.99–2.95 (1H, m),

2.79–2.71 (1H, m), 2.54–2.48 (1H, m), 2.30 (3H, s), 1.95–1.76 (2H, m), 1.15–1.13 (3H, d); LCMS  $m/z$  463 [M + H]<sup>+</sup>, 97.8% purity. **11b**: <sup>1</sup>H NMR (400 MHz, CDCl<sub>3</sub>) δ 8.03 (1H, s), 7.63–7.59 (2H, m), 7.44 (1H, s), 7.24–7.22 (1H, d), 7.10–7.06 (2H, t), 6.98–6.92 (3H, m), 4.58–4.53 (1H, q), 3.83 (3H, s), 3.27–3.22 (1H, m), 2.88–2.84 (1H, m), 2.75–2.71 (1H, m), 2.55–2.49 (1H, m), 2.31 (3H, s), 1.86–1.79 (2H, m), 1.37–1.35 (3H, d). LCMS  $m/z$  463 [M + H]<sup>+</sup>, 99.0% purity.

**(E)-(8-(3-Methoxy-4-(4-methyl-1H-imidazol-1-yl)benzylidene)-3-phenyl-5,6,7,8-tetrahydro-3H-[1,2,4]-oxadiazolo[4,3-a]pyridin-3-yl)methanol (20) and Its Enantiomer (20a)**. **20** and **20a** were prepared from **30c**, similar to the procedure for **5a** in method b. The racemate **20** was resolved on an OJ column, eluting with 65% isopropanol in hexanes to give **20a**. <sup>1</sup>H NMR (400 MHz, CDCl<sub>3</sub>): δ 7.71 (1H, s), 7.52–7.49 (2H, m), 7.46–7.39 (4H, m), 7.26–7.23 (1H, d), 7.00–6.97 (1H, d), 6.96 (1H, s), 6.92 (1H, s), 4.25–4.22 (1H, d), 4.10–4.07 (1H, d), 3.84 (3H, s), 3.39–3.33 (1H, m), 3.05–3.00 (1H, m), 2.73–2.70 (2H, m), 2.29 (3H, s), 2.00–1.84 (2H, m). LCMS  $m/z$  431 [M + 1]<sup>+</sup>, 100% purity.

**(E)-(3-(3-Fluorophenyl)-8-(3-methoxy-4-(4-methyl-1H-imidazol-1-yl)benzylidene)-5,6,7,8-tetrahydro-3H-[1,2,4]oxadiazolo[4,3-a]pyridin-3-yl)methanol (21) and Its Enantiomers (21a)**. **21** and **21a** were prepared from **30d**, similar to the procedure for **5a** in method b. Analytical data for **21a**: <sup>1</sup>H NMR (400 MHz, CDCl<sub>3</sub>) δ 7.73 (1H, s), 7.46 (1H, s), 7.43–7.38 (1H, m), 7.26–7.24 (3H, m), 7.12–7.07 (1H, m), 7.01–6.98 (1H, d), 6.97 (1H, s), 6.93 (1H, s), 4.22–4.19 (1H, d), 4.07–4.03 (1H, d), 3.85 (3H, s), 3.40–3.34 (1H, m), 3.06–3.01 (1H, m), 2.74–2.71 (2H, m), 2.30 (3H, s), 2.01–1.84 (2H, m). LCMS  $m/z$  449 [M + 1]<sup>+</sup>, 96.0% purity.

**(E)-(3-(2-Fluorophenyl)-8-(3-methoxy-4-(4-methyl-1H-imidazol-1-yl)benzylidene)-5,6,7,8-tetrahydro-3H-[1,2,4]oxadiazolo[4,3-a]pyridin-3-yl)methanol (22) and Its Enantiomers (22a)**. **22** and **22a** were prepared from **30e**, similar to the procedure for **5a** in method b. Analytical data for **22a**: <sup>1</sup>H NMR (400 MHz, CDCl<sub>3</sub>) δ 7.75–7.71 (2H, m), 7.44 (1H, s), 7.41–7.35 (1H, m), 7.25–7.21 (2H, m), 7.12–7.07 (1H, m), 6.99–6.92 (3H, m), 4.44–4.41 (1H, d), 4.06–4.03 (1H, d), 3.84 (3H, s), 3.52–3.47 (1H, m), 3.15–3.10 (1H, m), 2.83–2.75 (1H, m), 2.63–2.55 (1H, m), 2.29 (3H, s), 1.97–1.88 (2H, m). LCMS  $m/z$  449 [M + 1]<sup>+</sup>, 97.0% purity.

**(E)-4-(3-(Hydroxymethyl)-8-(3-methoxy-4-(4-methyl-1H-imidazol-1-yl)benzylidene)-5,6,7,8-tetrahydro-3H-[1,2,4]-oxadiazolo[4,3-a]pyridin-3-yl)benzylidene (23) and Its Enantiomer (23a)**. **23** and **23a** were prepared from **30f**, similar to the procedure for **5a** in method b. Analytical data for **23a**: <sup>1</sup>H NMR (400 MHz, CDCl<sub>3</sub>) δ 7.74–7.72 (3H, m), 7.65–7.63 (2H, d), 7.45 (1H, s), 7.26–7.24 (1H, d), 7.01–6.98 (1H, d), 6.96 (1H, s), 6.93 (1H, s), 4.24–4.21 (1H, d), 4.07–4.04 (1H, d), 3.85 (3H, s), 3.43–3.37 (1H, m), 3.05–2.99 (1H, m), 2.75–2.71 (2H, m), 2.30 (3H, s), 2.04–1.84 (2H, m). LCMS  $m/z$  456 [M + 1]<sup>+</sup>, 95.3% purity.

**(E)-(3-(3,5-Difluorophenyl)-8-(3-methoxy-4-(4-methyl-1H-imidazol-1-yl)benzylidene)-5,6,7,8-tetrahydro-3H-[1,2,4]-oxadiazolo[4,3-a]pyridin-3-yl)methanol (24) and Its Enantiomer (24a)**. **24** and **24a** were prepared from **30g**, similar to the procedure for **5a** in method b. The racemate **24** was resolved on an OD-H column by SFC using IPA as a cosolvent to give **24a**. <sup>1</sup>H NMR (400 MHz, CDCl<sub>3</sub>) δ 7.72 (1H, s), 7.45 (1H, s), 7.26–7.25 (1H, d), 7.06–7.04 (2H, m), 7.00–6.98 (1H, d), 6.96 (1H, s), 6.93 (1H, d), 6.87–6.82 (1H, m), 4.18–4.15 (1H, d), 4.04–4.01 (1H, d), 3.85 (3H, s), 3.43–3.37 (1H, m), 3.10–3.03 (1H, m), 2.74–2.71 (2H, m), 2.30 (3H, s), 2.00–1.85 (2H, m). LCMS  $m/z$  467 [M + 1]<sup>+</sup>, 100% purity.

**(E)-(8-(3-Methoxy-4-(4-methyl-1H-imidazol-1-yl)benzylidene)-3-(3,4,5-trifluorophenyl)-5,6,7,8-tetrahydro-3H-[1,2,4]oxadiazolo[4,3-a]pyridin-3-yl)methanol (25) and Its Enantiomer (25a)**. **25** and **25a** were prepared from **30h**, similar to the procedure for **5a** in method b. Analytical data for **25a**: <sup>1</sup>H NMR (500 MHz, CDCl<sub>3</sub>) δ 7.76 (1H, s), 7.46 (1H, s), 7.30–7.20 (3H, m), 7.01–6.96 (3H, m), 4.18–4.16 (1H, d), 4.10–4.08 (1H, d), 3.86 (3H, s), 3.46–3.40 (1H, m), 3.10–3.04 (1H, m), 2.80–2.60 (2H, m), 2.31 (3H, s), 2.00–1.95 (1H, m), 1.95–1.88 (1H, m). LCMS  $m/z$  485 [M + 1]<sup>+</sup>, 96.0% purity.

**(E)-(3-(5-Fluoropyridin-2-yl)-8-(3-methoxy-4-(4-methyl-1H-imidazol-1-yl)benzylidene)-5,6,7,8-tetrahydro-3H-[1,2,4]-oxadiazolo[4,3-a]pyridin-3-yl)methanol (26) and Its Enantiomer (26a)**. **26** and **26a** were prepared according to the similar

procedure for **5a** in method b from **30i** which was made from **45** according to the procedure for **30b**. The racemate **26** was resolved on an OJ column, eluting with 40% isopropanol in hexanes to give **26a**. <sup>1</sup>H NMR (400 MHz, CDCl<sub>3</sub>) δ 8.41 (1H, m), 7.84–7.81 (1H, m), 7.72 (1H, s), 7.53–7.48 (1H, m), 7.46 (1H, s), 7.26–7.23 (1H, d), 7.00–6.97 (1H, d), 6.96 (1H, s), 6.92 (1H, s), 4.45–4.42 (1H, d), 4.05–4.02 (1H, d), 3.84 (3H, s), 3.54–3.48 (1H, m), 3.19–3.14 (1H, m), 2.73–2.63 (2H, m), 2.29 (3H, s), 1.97–1.89 (1H, m), 1.83–1.75 (1H, m). LCMS  $m/z$  450 [M + H]<sup>+</sup>, 91.4% purity.

**(E)-(3-(5-Fluoropyridin-3-yl)-8-(3-methoxy-4-(4-methyl-1H-imidazol-1-yl)benzylidene)-5,6,7,8-tetrahydro-3H-[1,2,4]-oxadiazolo[4,3-a]pyridin-3-yl)methanol (27) and Its Enantiomer (27a)**. **27** and **27a** were prepared according to the similar procedure for **5a** in method b from **30j** which was made from **46** according to the procedure for **30b**. Analytical data for **27a**: <sup>1</sup>H NMR (400 MHz, CDCl<sub>3</sub>) δ 8.55–8.51 (2H, m), 7.72 (1H, s), 7.68–7.65 (1H, m), 7.46 (1H, s), 7.26–7.24 (1H, d), 7.00–6.93 (3H, m), 4.25–4.22 (1H, d), 4.10–4.07 (1H, d), 3.84 (3H, s), 3.46–3.40 (1H, m), 3.09–3.04 (1H, m), 2.75–2.70 (2H, m), 2.29 (3H, s), 2.05–1.85 (2H, m). LCMS  $m/z$  450 [M + H]<sup>+</sup>, 95% purity.

**3-Bromo-N-(1-(4-fluorophenyl)ethylidene)propan-1-amine (30a)**. Under N<sub>2</sub> protection, Et<sub>3</sub>N (40 mL, 29.0 mmol) was added slowly to a solution of 4-fluoroacetophenone (5 g, 36.2 mmol) and 3-bromopropan-1-amine hydrobromide (**41**) (10.3 g, 47.1 mmol) in anhydrous DMF (35 mL) and DCM (10 mL) while vigorously stirring. A solution of TiCl<sub>4</sub> (6.2 g, 32.6 mmol) in DCM (29 mL) was added dropwise at 0 °C. The reaction suspension was vigorously stirred at room temperature overnight. The reaction mixture was diluted with ether and filtered to remove solid. The filtrate was washed with ice cold brine 4 times and dried over anhydrous Na<sub>2</sub>SO<sub>4</sub> to give **30a** (6.8 g, 73.0% yield). The product was used without further purification in the preparation of **1**.

**Ethyl 2-(3-Bromopropylimino)-2-(4-fluorophenyl)acetate (30b)**. Under N<sub>2</sub> protection, the reaction solution of **42** (306.8 g, 1.1 mol), ethyl 2-(4-fluorophenyl)-2-oxoacetate (209 g, 1.1 mol), and trimethylsilyl trifluoromethanesulfonate (11.8 g, 0.05 mol) in DCM (1500 mL) was refluxed for 4 days, cooled to room temperature, washed with cold aqueous NaHCO<sub>3</sub> and brine, and dried over anhydrous Na<sub>2</sub>SO<sub>4</sub> to give **30b** (332 g, 98.6% yield). <sup>1</sup>H NMR (400 MHz, CDCl<sub>3</sub>): δ 7.71–7.67 (2H, m), 7.24–7.05 (2H, m), 4.45–4.39 (2H, q), 3.66–3.62 (2H, t), 3.55–3.52 (2H, t), 2.28–2.25 (2H, m), 1.41–1.37 (3H, t).

**Ethyl 4-(3-Bromopropyl)-3-((diethoxyphosphoryl)methyl)-5-(4-fluorophenyl)-4,5-dihydro-1,2,4-oxadiazole-5-carboxylate (31b)**. Under N<sub>2</sub> protection, NBS (101.3 g, 569 mmol) in DMF (240 mL) was added dropwise to a solution of diethyl 2-(hydroxyimino)ethylphosphonate (**28**) (111 g, 569 mmol) in DMF (470 mL) at –30 °C. The cooling bath was removed, and the reaction mixture was stirred for about 1 h to give **29** in DMF solution. This solution was slowly mixed with **30b** (178.8 g, 569 mmol) in DMF (400 mL) at –10 °C, followed by dropwise addition of Et<sub>3</sub>N (39.5 mL, 285 mmol) in DMF (250 mL) in an ice bath. The resulting reaction mixture was stirred at room temperature overnight. Additional 39.5 mL of Et<sub>3</sub>N in DMF (250 mL) was added dropwise in an ice bath, and the reaction mixture was stirred at room temperature for 4 h. Then an additional 1 equiv of **29** was made as described above and added dropwise to the reaction mixture in an ice bath, followed by slow addition of Et<sub>3</sub>N (79 mL) in two portions using the procedure described above. The reaction mixture was diluted with 70% EtOAc in hexanes and half-saturated NaCl in water. The aqueous phase was extracted with 70% EtOAc in hexanes. The combined organic phase was washed with a mixture of NaHCO<sub>3</sub> and NaCl in water, with half-saturated NaCl in water, and dried over anhydrous Na<sub>2</sub>SO<sub>4</sub>. The crude was purified on a silica gel column, eluting with EtOAc/hexanes in a gradient from 0% to 70% to give **31b** (122.6 g, 42.6% yield). <sup>1</sup>H NMR (400 MHz, CDCl<sub>3</sub>) δ 7.49–7.46 (2H, m), 7.12–7.07 (2H, m), 4.33–4.27 (2H, m), 4.21–4.16 (4H, m), 3.54–3.46 (1H, m), 3.42–3.34 (1H, m), 3.22–3.18 (2H, m), 2.99–2.93 (2H, m), 1.81–1.70 (1H, m), 1.62–1.51 (1H, m), 1.36–1.26 (9H, m).

**Ethyl 8-(Diethoxyphosphoryl)-3-(4-fluorophenyl)-5,6,7,8-tetrahydro-3H-[1,2,4]oxadiazolo[4,3-a]pyridine-3-carboxylate (32b)**. Under N<sub>2</sub> protection, *t*-BuOK (29.7 g, 265.0 mmol) in

anhydrous THF (265 mL) was added dropwise to a solution of **31b** (122.6 g, 240.9 mmol) in anhydrous THF (2400 mL) at  $-70^{\circ}\text{C}$ . The reaction mixture was allowed to warm to  $12^{\circ}\text{C}$  over a period of 2 h, diluted with brine, and extracted with EtOAc. The combined organic phase was washed with brine and dried over anhydrous  $\text{Na}_2\text{SO}_4$ . The crude was purified on a silica gel column, eluting with EtOAc/hexanes in a gradient from 0% to 100% to give **32b** (82.6 g, 80.1% yield), a mixture of diastereomers A and B. The analytical diastereomer samples were obtained by purification on silica gel column again.  $^1\text{H}$  NMR (400 MHz,  $\text{CDCl}_3$ ), diastereomer A:  $\delta$  7.45–7.41 (2H, m), 7.08–7.04 (2H, m), 4.30–4.12 (6H, m), 3.33–3.28 (1H, m), 3.13–3.05 (1H, tt), 2.79–2.74 (1H, m), 2.13–1.75 (4H, m), 1.34–1.26 (9H, m). Diastereomer B:  $\delta$  7.45–7.41 (2H, m), 7.10–7.05 (2H, m), 4.33–4.14 (6H, m), 3.42–3.37 (1H, m), 3.15–3.06 (1H, tt), 2.62–2.56 (1H, m), 2.18–2.08 (2H, m), 1.92–1.78 (1H, m), 1.68–1.57 (1H, m), 1.36–1.27 (9H, m).

**(S,E)-1-(3-(4-Fluorophenyl)-8-(3-methoxy-4-(4-methyl-1H-imidazol-1-yl)benzylidene)-5,6,7,8-tetrahydro-3H-[1,2,4]-oxadiazolo[4,3-a]pyridin-3-yl)ethanone (33)**. A solution of 3 M MeMgBr in ether (3.4 mL, 10.3 mmol) and  $\text{Et}_3\text{N}$  (4.3 mL, 31 mmol) in THF (6.8 mL) was added dropwise to a stirred solution of **3a** (2.5 g, 5.2 mmol) in 15.6 mL of THF at  $-60^{\circ}\text{C}$  under nitrogen atmosphere. The reaction mixture was allowed to warm to  $10^{\circ}\text{C}$  over a period of 5 h, stirred for an additional 1 h at room temperature, quenched with a mixture of brine and ice, diluted with EtOAc, filtered through a Celite pad, and extracted with EtOAc. The combined organic phase was washed with brine and dried over anhydrous  $\text{Na}_2\text{SO}_4$ . The crude was purified on a silica gel column, eluting with EtOAc/hexanes from 0% to 75% to give a crude of **33** (1.7 g) containing 50% of **3a**. This crude was used without further purification in the preparation of **11a** and **11b**. The analytical sample was purified on a C18 column, eluting with MeCN/water containing 0.1% formic acid.  $^1\text{H}$  NMR (400 MHz,  $\text{CDCl}_3$ ):  $\delta$  7.67 (1H, s), 7.47–7.43 (3H, m), 7.21–7.19 (1H, d), 7.12–7.08 (2H, t), 6.96–6.94 (1H, d), 6.92 (1H, s), 6.88 (1H, s), 3.80 (3H, s), 3.58–3.53 (1H, m), 2.83–2.77 (1H, m), 2.70–2.59 (2H, m), 2.25–2.24 (6H, ss), 1.92–1.87 (1H, m), 1.72–1.66 (1H, m).

**(S,E)-3-(4-Fluorophenyl)-8-(3-methoxy-4-(4-methyl-1H-imidazol-1-yl)benzylidene)-5,6,7,8-tetrahydro-3H-[1,2,4]-oxadiazolo[4,3-a]pyridine-3-carbaldehyde (34)**. Under  $\text{N}_2$  protection, DMSO (0.16 mL, 2.2 mmol) was added dropwise to a solution of oxalyl dichloride (0.11 mL, 1.3 mmol) in anhydrous DCM (11.1 mL) at  $-78^{\circ}\text{C}$ , followed by dropwise addition of **5a** (500 mg, 1.1 mmol) in anhydrous DCM (1.5 mL). After the mixture was stirred at  $-78^{\circ}\text{C}$  for 1 h,  $\text{Et}_3\text{N}$  (0.62 mL, 4.5 mmol) was added dropwise. The reaction mixture was stirred for 30 min, allowed to warm to room temperature, diluted with cold brine, and extracted with DCM. The combined organic phase was washed with brine, dried over anhydrous  $\text{Na}_2\text{SO}_4$ , and concentrated under reduced pressure to give **34** (507 mg), which was used without further purification in the preparations of **36**, **37**, and **38**. MS  $m/z$  447.

**(S,E)-3-(4-Fluorophenyl)-8-(3-methoxy-4-(4-methyl-1H-imidazol-1-yl)benzylidene)-3-(methoxymethyl)-5,6,7,8-tetrahydro-3H-[1,2,4]-oxadiazolo[4,3-a]pyridine (35)**. Sodium hydride (2 mg, 60% in mineral oil) and methyl iodide (16.6 mg, 0.12 mmol) were added to a stirred solution of **5a** (7.5 mg, 0.017 mmol) in anhydrous DMF (0.2 mL) at room temperature under nitrogen atmosphere. The reaction mixture was stirred for 15 min, quenched with iced brine, and extracted with EtOAc. The organic phase was dried over anhydrous  $\text{Na}_2\text{SO}_4$  and concentrated. The crude was purified on a C18 column with MeCN/water containing 0.1% formic acid. The desired fraction was neutralized with aqueous  $\text{NaHCO}_3$ , concentrated under reduced pressure to remove MeCN, and extracted with EtOAc to give **35**.  $^1\text{H}$  NMR (400 MHz,  $\text{CDCl}_3$ ):  $\delta$  8.05 (1H, s), 7.55–7.51 (2H, m), 7.46 (1H, s), 7.26–7.24 (1H, d), 7.11–7.06 (2H, t), 7.02–6.93 (3H, m), 4.04–4.01 (1H, d), 3.96–3.93 (1H, d), 3.84 (3H, s), 3.50 (3H, s), 3.29–3.26 (1H, m), 2.97–2.94 (1H, m), 2.71–2.68 (2H, m), 2.33 (3H, s), 1.95–1.85 (1H, m), 1.85–1.75 (1H, m). LCMS  $m/z$  463  $[\text{M} + \text{H}]^+$ , 98.5% purity.

**(S,E)-1-(3-(4-Fluorophenyl)-8-(3-methoxy-4-(4-methyl-1H-imidazol-1-yl)benzylidene)-5,6,7,8-tetrahydro-3H-[1,2,4]-oxadiazolo[4,3-a]pyridin-3-yl)-N-methylmethanamine (36)**. Sodium triacetoxy borohydride (252 mg, 1.2 mmol) was slowly

added to a stirred reaction mixture of **34** (200 mg, 0.45 mmol), 2 M solution methylamine in THF (0.5 mL, 1 mmol), and acetic acid (0.051 mL, 0.9 mmol) in DCE (12 mL) at  $0^{\circ}\text{C}$  under nitrogen atmosphere. The reaction mixture was stirred at room temperature overnight, quenched with aqueous  $\text{NaHCO}_3$ , and extracted with EtOAc. The organic phase was dried over  $\text{Na}_2\text{SO}_4$  and concentrated under reduced pressure. The crude was purified on a C18 column with MeCN/water containing 0.1% formic acid. The desired fraction was neutralized with aqueous  $\text{NaHCO}_3$ , concentrated under reduced pressure, and extracted with EtOAc to give **36** (87.9 mg, 42.5% yield).  $^1\text{H}$  NMR (400 MHz,  $\text{CDCl}_3$ ):  $\delta$  9.15 (1H, s), 7.44–7.36 (3H, m), 7.13–7.09 (2H, t), 7.05 (1H, s), 6.94 (1H, s), 6.79 (1H, s), 6.73–6.71 (1H, d), 3.99–3.95 (1H, d), 3.82 (3H, s), 3.72–3.69 (1H, d), 3.44–3.38 (1H, m), 2.93 (3H, s), 2.76–2.67 (2H, m), 2.44 (3H, s), 2.39–2.32 (1H, m), 1.99–1.87 (1H, m), 1.73–1.61 (1H, m). LCMS  $m/z$  462  $[\text{M} + \text{H}]^+$ , 99.9% purity.

**(S,E)-1-(3-(4-Fluorophenyl)-8-(3-methoxy-4-(4-methyl-1H-imidazol-1-yl)benzylidene)-5,6,7,8-tetrahydro-3H-[1,2,4]-oxadiazolo[4,3-a]pyridin-3-yl)-N,N-dimethylmethanamine (37)**. **37** was made from **34** and dimethylamine according to the procedure for **36**.  $^1\text{H}$  NMR (400 MHz,  $\text{CDCl}_3$ ):  $\delta$  7.69 (1H, s), 7.54–7.50 (2H, m), 7.46 (1H, s), 7.22–7.20 (1H, d), 7.09–7.05 (3H, t), 6.97–6.95 (1H, d), 6.94 (1H, s), 6.91 (1H, s), 3.82 (3H, s), 3.23–3.18 (1H, m), 3.09–3.05 (1H, d), 2.95–2.91 (1H, d), 2.85–2.79 (1H, m), 2.76–2.70 (1H, m), 2.60–2.52 (1H, m), 2.50 (6H, s), 2.28 (3H, s), 1.90–1.79 (2H, m). LCMS  $m/z$  476  $[\text{M} + \text{H}]^+$ , 98.1% purity.

**(S,E)-2-((3-(4-Fluorophenyl)-8-(3-methoxy-4-(4-methyl-1H-imidazol-1-yl)benzylidene)-5,6,7,8-tetrahydro-3H-[1,2,4]-oxadiazolo[4,3-a]pyridin-3-yl)methylamino)ethanol (38)**. **38** was made from **34** and 2-aminoethyl benzoate according to the procedure for **36**, followed by hydrolysis of the benzoate with lithium hydroxide.  $^1\text{H}$  NMR (400 MHz,  $\text{CDCl}_3$ ):  $\delta$  9.03 (1H, s), 7.45–7.41 (2H, m), 7.35–7.33 (1H, d), 7.15–7.09 (3H, m), 7.05 (1H, s), 6.88 (1H, s), 6.81–6.79 (1H, d), 4.20–4.17 (1H, d), 4.02–3.97 (2H, m), 3.85 (3H, s), 3.66–3.63 (1H, d), 3.46–3.43 (2H, m), 3.39–3.35 (1H, m), 2.76–2.70 (2H, m), 2.45 (3H, s), 2.37–2.29 (1H, m), 1.94–1.86 (1H, m), 1.75–1.69 (1H, m). LCMS  $m/z$  492  $[\text{M} + \text{H}]^+$ , 99.4% purity.

**(S,E)-N-((3-(4-Fluorophenyl)-8-(3-methoxy-4-(4-methyl-1H-imidazol-1-yl)benzylidene)-5,6,7,8-tetrahydro-3H-[1,2,4]-oxadiazolo[4,3-a]pyridin-3-yl)methyl)-N-methylacetamide (39)**. Acetic anhydride (5.3 mg, 0.052 mmol) in DCM (0.1 mL) was added dropwise to a stirred reaction mixture of **36** (20 mg, 0.043 mmol) and  $\text{Et}_3\text{N}$  (0.02 mL) in anhydrous DCM (0.4 mL) at  $0^{\circ}\text{C}$  under nitrogen atmosphere. The reaction mixture was stirred for 30 min, allowed to warm to room temperature, quenched with water, concentrated to remove DCM, and purified on a C18 column, eluting with MeCN/water containing 0.1% formic acid. The desired fraction was neutralized with aqueous  $\text{NaHCO}_3$ , concentrated under reduced pressure, and extracted with EtOAc to give **39** (9.4 mg, 43.1%).  $^1\text{H}$  NMR (400 MHz,  $\text{CDCl}_3$ ):  $\delta$  7.69 (1H, s), 7.58–7.55 (2H, m), 7.44 (1H, s), 7.23–7.21 (1H, d), 7.11–7.07 (2H, t), 6.98–6.94 (2H, m), 6.90 (1H, s), 4.86–4.82 (1H, d), 3.82 (3H, s), 3.53–3.49 (1H, m), 3.47–3.43 (1H, d), 3.22 (3H, s), 2.79–2.72 (1H, m), 2.63–2.57 (1H, m), 2.45–2.37 (1H, m), 2.28 (3H, s), 2.09 (3H, s), 1.80–1.70 (2H, m). LCMS  $m/z$  504  $[\text{M} + \text{H}]^+$ , 100% purity.

**(S,E)-N-((3-(4-Fluorophenyl)-8-(3-methoxy-4-(4-methyl-1H-imidazol-1-yl)benzylidene)-5,6,7,8-tetrahydro-3H-[1,2,4]-oxadiazolo[4,3-a]pyridin-3-yl)methyl)-N-methylmethanesulfonamide (40)**. **40** was made from methanesulfonyl chloride according to the procedure for **39** in 46.6% yield.  $^1\text{H}$  NMR (400 MHz,  $\text{CDCl}_3$ ):  $\delta$  7.94 (1H, s), 7.54–7.51 (2H, m), 7.45 (1H, s), 7.24–7.22 (1H, d), 7.13–7.09 (2H, t), 6.99–6.96 (2H, m), 6.93 (1H, s), 4.28–4.24 (1H, d), 3.84 (3H, s), 3.47–3.43 (1H, d), 3.43–3.39 (1H, m), 3.11 (3H, s), 2.84 (3H, s), 2.82–2.78 (1H, m), 2.73–2.66 (1H, m), 2.45–2.39 (1H, m), 2.32 (3H, s), 1.90–1.80 (2H, m). LCMS  $m/z$  540  $[\text{M} + \text{H}]^+$ , 96.0% purity.

**N-(3-Bromopropyl)-N,N-bis(trimethylsilyl)amine (42)**. Chlorotrimethylsilane (273 g, 2.5 mol) was added to a suspension of **41** in anhydrous DCM (3000 mL) in an ice bath, followed by slow addition of  $\text{Et}_3\text{N}$  (525 mL, 3.8 mol). The reaction mixture was stirred at room temperature overnight and filtered to remove white solid. The filtrate was concentrated under reduced pressure, diluted with ether, filtered,

and concentrated again to give **42** (306.8 g, 95.1% yield). The product was used without further purification in the preparation of **30b**.

**Ethyl 2-(5-Fluoropyridin-2-yl)-2-oxoacetate (45)**. Isopropylmagnesium chloride–lithium chloride complex (1.3 M in THF) (131 mL, 170.5 mmol) was added slowly to a solution of 2-bromo-5-fluoropyridine (**43**) (25 g, 142.1 mmol) in 200 mL of THF over 20 min at 0 °C. The resulting mixture was allowed to warm to room temperature over 1 h and stirred at room temperature for 30 min. The prepared organometallic solution was added to a solution of diethyl oxalate (22.7 g, 135 mmol) in 100 mL of THF at –78 °C slowly via cannulation. The reaction mixture was allowed to warm to room temperature overnight, quenched with saturated NH<sub>4</sub>Cl, and extracted with ether. The combined organic layers were dried over anhydrous Na<sub>2</sub>SO<sub>4</sub>, filtered, and concentrated to dryness. The residue was purified on a silica gel column, eluting with EtOAc/hexanes in a gradient from 0% to 100% to give **45** (13 g, 47% yield). <sup>1</sup>H NMR (400 MHz, CDCl<sub>3</sub>): δ 8.57 (1H, m), 8.19–8.15 (1H, m), 7.62–7.57 (1H, m), 4.50–4.45 (2H, q), 1.42–1.38 (3H, t).

**Ethyl 2-(5-Fluoropyridin-3-yl)-2-oxoacetate (46)**. **46** was prepared from 3-bromo-5-fluoropyridine (**44**) according to the procedure for **45**. The product was used without further purification in the preparation of **30j**.

**(S)-2-Amino-2-(3,4,5-trifluorophenyl)ethanol (48)**. Sodium hydroxide (8.2 g, 205 mmol) in water (300 mL) was added to a solution of CbzNH<sub>2</sub> (31.5 g, 208 mmol) in PrOH (300 mL). The mixture was stirred for 3 min, followed by dropwise addition of *tert*-butyl hypochlorite (23.5 mL, 205 mmol). After this mixture was stirred for another 6 min, a solution of (DHQ)<sub>2</sub>PHAL (600 mg, 0.75 mmol) and 1,2,3-trifluoro-5-vinylbenzene **47** (100 mmol) in PrOH (150 mL) was added, followed by addition of K<sub>2</sub>OsO<sub>2</sub>(OH)<sub>4</sub> (380 mg, 1.0 mmol). The resulting mixture turned green immediately. Stirring was continued for 2 h, upon which the solution turned light yellow. The reaction was quenched by stirring the mixture with an excess of Na<sub>2</sub>S<sub>2</sub>O<sub>3</sub> for 2 h. The PrOH layer was then separated and concentrated in vacuum. The solid residue was dissolved in EtOAc, which was passed through a silica gel pad, and concentrated. The residue was treated with 15% EtOAc/hexanes to remove solid CbzNH<sub>2</sub>. The filtrate was reconcentrated and crystallized in EtOAc/hexanes to give an undesired regioisomer (3 g). The filtrate was concentrated again to provide a solid mixture (18 g) with the desired Cbz-protected regioisomer as the major component (>70%). This mixture was directly subjected to hydrogenation catalyzed with Pd(OH)<sub>2</sub>/C (9 g, 50% water, 20% Pd on dry basis) in MeOH (250 mL) for 1 h. The reaction mixture was filtered through Celite and concentrated to give **48** (8.6 g, 45.0% yield), which was used without further purification in the preparation of **51**.

**(S,E)-1-(2-Hydroxy-1-(3,4,5-trifluorophenyl)ethyl)-3-(3-methoxy-4-(4-methyl-1H-imidazol-1-yl)benzylidene)piperidin-2-one (51)**. **51** was prepared from **48** and (*E*)-5-chloro-2-(3-methoxy-4-(4-methyl-1H-imidazol-1-yl)benzylidene)pentanoic acid TFA salt (**49**) using a similar method described in the ref 13. <sup>1</sup>H NMR (400 MHz, CDCl<sub>3</sub>): δ 7.82 (1H, s), 7.70 (1H, s), 7.24–7.22 (1H, d), 7.00–6.91 (4H, m), 6.92 (1H, s), 5.78–5.76 (1H, m), 4.2–4.05 (2H, m), 3.84 (3H, s), 3.42–3.35 (1H, m), 3.20–3.12 (1H, m), 2.88–2.76 (2H, m), 2.28 (3H, s), 1.90–1.70 (2H, m). LCMS *m/z* 472 [M + H]<sup>+</sup>, 96.8% purity.

**(S,E)-1-(2-(Aminoxy)-1-(3,4,5-trifluorophenyl)ethyl)-3-(3-methoxy-4-(4-methyl-1H-imidazol-1-yl)benzylidene)piperidin-2-one (52)**. Under N<sub>2</sub> protection, DIAD (3.0 g, 15 mmol) was added dropwise to a mixture of **51** (4.7 g, 10 mmol), PPh<sub>3</sub> (3.9 g, 15 mmol), and *N*-hydroxyphthalimide (2.4 g, 15 mmol) in anhydrous THF (100 mL) at –10 °C. The mixture was allowed to warm to room temperature and stirred for 30 min. After evaporation of THF, the residue was dissolved in EtOAc, washed with aqueous NaHCO<sub>3</sub>, dried over anhydrous Na<sub>2</sub>SO<sub>4</sub>, and concentrated. The residue was then treated with NH<sub>2</sub>NH<sub>2</sub> monohydrate (1.0 g, 20 mmol) in EtOH (100 mL) overnight. After evaporation of EtOH, the residue was dissolved in DCM, washed consecutively with water and brine, and dried over anhydrous Na<sub>2</sub>SO<sub>4</sub>. The DCM was then removed and the residue was purified on a silica gel column, eluting with MeOH/DCM containing 0.1% Et<sub>3</sub>N to afford **52** (3.5 g, 72.2%). <sup>1</sup>H NMR

(400 MHz, CDCl<sub>3</sub>): δ 7.86 (1H, br s), 7.71 (1H, s), 7.25–7.23 (1H, m), 7.05–7.02 (2H, m), 6.95–6.92 (3H, m), 6.33–6.28 (1H, br t), 5.70 (2H, br s), 4.13–4.10 (2H, m), 3.84 (3H, s), 3.32–3.25 (1H, m), 3.07–3.02 (1H, m), 2.92–2.75 (2H, m), 2.28 (3H, s), 1.92–1.85 (1H, m), 1.78–1.70 (1H, m).

**(S,E)-9-(3-Methoxy-4-(4-methyl-1H-imidazol-1-yl)benzylidene)-4-(3,4,5-trifluorophenyl)-3,4,6,7,8,9-hexahydroprido[2,1-c][1,2,4]oxadiazine (53)**. A solution of **52** (2.7 g, 5.5 mmol) in EtOH (30 mL) was added to a mixture of P<sub>2</sub>O<sub>5</sub> (7.5 g, 52.8 mmol) in EtOH (35 mL). The resulting mixture was then stirred at 80 °C overnight, cooled to room temperature, and diluted with DCM and water. Aqueous K<sub>2</sub>CO<sub>3</sub> was added to adjust the pH to ~9–10. The organic layer was then collected and dried over anhydrous Na<sub>2</sub>SO<sub>4</sub>. After the DCM was evaporated, the residue was purified on a silica gel column, eluting with MeOH/DCM containing 0.1% Et<sub>3</sub>N to afford **53** (2.2 g, 84.6% yield). <sup>1</sup>H NMR (400 MHz, CDCl<sub>3</sub>): δ 7.69 (1H, s), 7.51 (1H, br s), 7.24–7.21 (1H, m), 7.00–6.95 (4H, m), 6.91 (1H, s), 4.26–4.24 (1H, m), 4.04–4.02 (2H, m), 3.83 (3H, s), 3.18–3.03 (2H, m), 2.86–2.79 (1H, m), 2.75–2.68 (1H, m), 2.28 (3H, s), 1.93–1.75 (2H, m). LCMS *m/z* 469 [M + H]<sup>+</sup>, 96.6% purity, 90% ee.

## AUTHOR INFORMATION

### Corresponding Author

\*For Z.-Y.S.: phone, +1 917 657 6061; e-mail, ZYSUN66011@yahoo.com. For Z.Z.: phone, +1 732 822 7384; e-mail johnnyzzhu@msn.com.

## ACKNOWLEDGMENTS

We thank Mary Humphries, Matthew Nienart, and Kathryn Galvin for conducting the *in vivo* portion of the cynomolgous study; Alexei Buevich, Rebecca Osterman, Mary Senior, and Tze-Ming Chan for NMR structural analysis; Steve Sorota for all hERG cellular data; and Jessie Wong, Xian Liang, Yan Jin, Teresa Andreani, Yang Cao, and Michael Starks for scale-up and chiral separation.

## DEDICATION

<sup>†</sup>This paper is dedicated to Professor Ronald Breslow on the occasion of his 80th birthday.

## ABBREVIATIONS USED

GSM,  $\gamma$ -secretase modulator; AD, Alzheimer's disease; CNS, central nervous system; GSI,  $\gamma$ -secretase inhibitor; APP, amyloid precursor protein; NSAID, nonsteroidal anti-inflammatory drug;  $\alpha\beta$ , amyloid  $\beta$ ; BACE,  $\beta$ -site amyloid cleaving enzyme; CSF, cerebral spinal fluid; HEK, human embryonic kidney cell; PBS, phosphate buffered saline

## REFERENCES

- (1) Wimo, A.; Prince, M. World Alzheimer Report 2010: The Global Economic Impact of Dementia; Alzheimer's Disease International (ADI): London, U.K., September 2010.
- (2) (a) Yan, R.; Bienkowski, M. J.; Shuck, M. E.; Miao, H.; Tory, M. C.; Pauley, A. M.; Brashler, J. R.; Stratman, N. C.; Mathews, W. R.; Buhl, A. E.; Carter, D. B.; Tomasselli, A. G.; Parodi, L. A.; Heinrikson, R. L.; Gurney, M. E. Membrane-anchored aspartyl protease with Alzheimer's disease  $\beta$ -secretase specificity. *Nature* **1999**, *402*, 533–537. (b) Vassar, R.; Bennett, B. D.; Babu-Khan, S.; Kahn, S.; Mendiaz, E. A.; Denis, P.; Teplow, D. B.; Ross, S.; Amarante, P.; Loeloff, R.; Luo, Y.; Fisher, S.; Fuller, J.; Edenson, S.; Lile, J.; Jarosinski, M. A.; Biere, A. L.; Curran, E.; Burgess, T.; Louis, J.-C.; Collins, F.; Treanor, J.; Rogers, G.; Citron, M.  $\beta$ -Secretase cleavage of Alzheimer's amyloid precursor protein by the transmembrane aspartic protease BACE. *Science* **1999**, *286*, 735–741. (c) Hussain, I.; Powell, D.; Howlett, D. R.; Tew, D. G.; Meek, T. D.; Chapman, C.; Gloger, I. S.; Murphy, K. E.;

- Southan, C. D.; Ryan, D. M.; Smith, T. S.; Simmons, D. L.; Walsh, F. S.; Dingwall, C.; Christie, G. Identification of a novel aspartic protease (Asp 2) as beta-secretase. *Mol. Cell. Neurosci.* **1999**, *14*, 419–427.
- (d) Sinha, S.; Anderson, J. P.; Barbour, R.; Basi, G. S.; Caccavello, R.; Davis, D.; Doan, M.; Dovey, H. F.; Frigon, N.; Hong, J.; Jacobson-Croak, K.; Jewett, N.; Keim, P.; Knops, J.; Lieberburg, L.; Power, M.; Tan, H.; Tatsuno, G.; Tung, J.; Schenk, D.; Seubert, P.; Suomensaar, S. M.; Wang, S.; Walker, D.; Zhao, J.; McConlogue, L.; Varghese, J. Purification and cloning of amyloid precursor protein  $\beta$ -secretase from human brain. *Nature* **1999**, *402*, 537–540.
- (3) Guardia-Laguarta, C.; Pera, M.; Lleó, A.  $\gamma$ -Secretase as a therapeutic target in Alzheimer's disease. *Curr. Drug Targets* **2010**, *11*, 506–517.
- (4) (a) Hardy, J. A.; Higgins, G. A. Alzheimer's disease: the amyloid cascade hypothesis. *Science* **1992**, *256*, 184–185. (b) Hardy, J.; Selkoe, D. J. The amyloid hypothesis of Alzheimer's disease: progress and problem on the road to therapeutics. *Science* **2002**, *297*, 353–356. (c) Walsh, D. M.; Selkoe, D. J.  $A\beta$  oligomers: a decade of discovery. *J. Neurochem.* **2007**, *101*, 1172–1184.
- (5) Artavanis-Tsakonas, S.; Rand, M. D.; Lake, R. J. Notch signaling: cell fate control and signal integration in development. *Science* **1999**, *284*, 770–776.
- (6) Hüll, M.; Berger, M.; Heneka, M. Disease-modifying therapies in Alzheimer's disease. *Drug* **2006**, *66*, 2075–2093.
- (7) (a) Siemers, E. R.; Quinn, J. F.; Kaye, J.; Farlow, M. R.; Porsteinsson, A.; Tariot, P.; Zoulnouni, P.; Galvin, J. E.; Holtzman, D. M.; Knopman, D. S.; Satterwhite, J.; Gonzales, C.; Dean, R. A.; May, P. C. Effects of a  $\gamma$ -secretase inhibitor in a randomized study of patients with Alzheimer disease. *Neurology* **2006**, *66*, 602–604. (b) Fleisher, A. S.; Raman, R.; Siemers, E. R.; Becerra, L.; Clark, C. M.; Dean, R. A.; Farlow, M. R.; Galvin, J. E.; Peskind, E. R.; Quinn, J. F.; Sherzai, A.; Sowell, B. B.; Aisen, P. S.; Thal, L. J. Phase 2 safety trial targeting amyloid  $\beta$  production with a  $\gamma$ -secretase inhibitor in Alzheimer disease. *Arch. Neurol.* **2008**, *65*, 1031–1038. (c) Siemers, E.; Skinner, M.; Dean, R. A.; Gonzales, C.; Satterwhite, J.; Farlow, M.; Ness, D.; May, P. C. Safety, tolerability, and changes in amyloid  $\beta$  concentrations after administration of a  $\gamma$ -secretase inhibitor in volunteers. *Clin. Neuropharmacol.* **2007**, *28*, 126–132. (d) Bateman, R. J.; Siemers, E. R.; Mawuenyega, K. G.; Wen, G.; Browning, K. R.; Sigurdson, W. C.; Yarasheski, K. E.; Friedrich, S. W.; DeMattos, R. B.; May, P. C.; Paul, S. M.; Holtzman, D. M. A  $\gamma$ -secretase inhibitor decreases amyloid- $\beta$  production in the central nervous system. *Ann. Neurol.* **2009**, *66*, 48–64. (e) Carlson, C.; Estergard, W.; Oh, J.; Suh, J.; Jack, C. R. Jr.; Siemers, E.; Barakos, J. Prevalence of asymptomatic vasogenic edema in pretreatment Alzheimer's disease study cohorts from phase 3 trials of semagacestat and solanezumab. *Alzheimer's Dementia* **2011**, *7*, 396–401.
- (8) (a) Weggen, S.; Eriksen, J.; Das, P.; Saqi, S. A.; Wang, R.; Pietrzik, C. U.; Findlay, K. A.; Smith, T. E.; Murphy, M. P.; Bulter, T.; Kang, D. E.; Marquez-Sterling, N.; Golde, T. E.; Koo, E. H. A subset of NSAIDs lower amyloidogenic  $A\beta$ 42 independently of cyclooxygenase activity. *Nature* **2001**, *414*, 212–216. (b) Kukar, T.; Murphy, M. P.; Eriksen, J. L.; Sagi, S. A.; Weggen, S.; Smith, T. E.; Ladd, T.; Khan, M. A.; Kache, R.; Beard, J.; Dodson, M.; Merit, S.; Ozols, V. V.; Anastasiadis, P. Z.; Das, P.; Fauq, A.; Koo, E. H.; Golde, T. E. Diverse compounds mimic Alzheimer disease-causing mutations by augmenting  $A\beta$ 42 production. *Nat. Med.* **2005**, *11*, 545–550. (c) Pettersson, M.; Kauffman, G. W.; am Ende, C. W.; Patel, N. C.; Stiff, C.; Tran, T. P.; Johnson, D. S. Novel  $\gamma$ -secretase modulators: a review of patents from 2008 to 2010. *Expert Opin. Ther. Pat.* **2011**, *21*, 205–226. (d) Czirr, E.; Weggen, S.  $\gamma$ -Secretase modulation with  $A\beta$ 42-lowering nonsteroidal anti-inflammatory drugs and derived compounds. *Neurodegener. Dis.* **2006**, *3*, 298–304. (e) Oehlrich, D.; Berthelot, D. J.-C.; Gijzen, H. J. M.  $\gamma$ -Secretase modulators as potential disease modifying anti-Alzheimer's drugs. *J. Med. Chem.* **2011**, *54*, 669–698. (f) Olson, R. E.; Marcin, L. R. Secretase inhibitors and modulators for the treatment of Alzheimer's disease. *Annu. Rep. Med. Chem.* **2007**, *42*, 27–47. (g) Imbimbo, B. P.; Giardina, G. A. M.  $\gamma$ -Secretase inhibitors and modulators for the treatment of Alzheimer's disease: disappointments and hopes. *Curr. Top. Med. Chem.* **2011**, *11*, 1555–1570. (h) Schmidt, B.; Baumann, S.; Braun, H. A.; Larbig, G. Inhibitors and modulators of  $\beta$ - and  $\gamma$ -secretase. *Curr. Top. Med. Chem.* **2006**, *6*, 377–392.
- (9) Kounnas, M. Z.; Danks, A. M.; Cheng, S.; Tyree, C.; Ackerman, E.; Zhang, X.; Ahn, K.; Nguyen, P.; Comer, D.; Mao, L.; Yu, C.; Pleyntet, D.; Digregorio, P. J.; Velicelebi, G.; Stauderman, K. A.; Comer, W. T.; Mobley, W. C.; Li, Y.-M.; Sisodia, S. S.; Tanzi, R. E.; Wagner, S. L. Modulation of  $\gamma$ -secretase reduces  $\beta$ -amyloid deposition in a transgenic mouse model of Alzheimer's disease. *Neuron* **2010**, *67*, 769–780.
- (10) (a) Kim, J.; Onstead, L.; Randle, S.; Price, R.; Smithson, L.; Zwizinski, C.; Dickson, D. W.; Golde, T.; McGowan, E.  $A\beta$ 40 inhibits amyloid deposition in vivo. *J. Neurosci.* **2007**, *27*, 627–633. (b) Chen, Y.; Dong, C.  $A\beta$ 40 promotes neuronal cell fate in neural progenitor cells. *Cell Death Differ.* **2009**, *16*, 386–394. (c) Abramov, E.; Dolev, I.; Fogel, H.; Ciccotosto, G. D.; Ruff, E.; Slutsky, I. Amyloid- $\beta$  as a positive endogenous regulator of release probability at hippocampal synapses. *Nat. Neurosci.* **2009**, *12*, 1567–1576. (d) Wang, R.; Wang, B.; He, W.; Zheng, H. Wild-type presenilin 1 protects against Alzheimer disease mutation-induced amyloid pathology. *J. Biol. Chem.* **2006**, *281*, 15330–15336.
- (11) (a) Imbimbo, B. P. Why did tarenfluril fail in Alzheimer's disease? *J. Alzheimer's Dis.* **2009**, *17*, 757–760. (b) Eriksen, J. L.; Sagi, S. A.; Smith, T. E.; Weggen, S.; Das, P.; McLendon, D. C.; Ozols, V. V.; Jessing, K. W.; Zavitz, K. H.; Koo, E. H.; Golde, T. E. NSAIDs and enantiomers of flurbiprofen target  $\gamma$ -secretase and lower  $A\beta$ 42 in vivo. *J. Clin. Invest.* **2003**, *112*, 440–449.
- (12) Cheng, S.; Comer, D. D.; Mao, L.; Balow, G. P.; Pleyntet, D. Aryl Compounds and Uses Thereof in Modulating Amyloid  $\beta$ . WO 2004110350, 2004.
- (13) Kimura, T.; Kawano, K.; Doi, E.; Kitazawa, N.; Shin, K.; Miyagawa, T.; Kaneko, T.; Ito, K.; Takaishi, M.; Sasaki, T.; Hagiwara, H. Cinnamide Compound. US 20060004013, 2006.
- (14) Kimura, T.; Kawano, K.; Doi, E.; Kitazawa, N.; Takaishi, M.; Ito, K.; Kaneko, T.; Sasaki, T.; Sato, N.; Miyagawa, T.; Hagiwara, H. Morpholine Type Cinnamide Compound. US20070117798, 2007.
- (15) Gustafsson, D.; Nyström, J.-E.; Carlsson, S.; Bredberg, U.; Eriksson, U.; Gyzander, E.; Elg, M.; Antonsson, T.; Hoffmann, K.-J.; Ungell, A.-L.; Sörensen, H.; Nägård, S.; Abrahamsson, A.; Bylund, R. The direct thrombin inhibitor melagatran and its oral prodrug H 376/95: intestinal absorption properties, biochemical and pharmacodynamic effects. *Thromb. Res.* **2001**, *101*, 171–181.
- (16) Tomczuk, B.; Lu, T.; Soll, R. M.; Fedde, C.; Wang, A.; Murphy, L.; Cryslar, C.; Dasgupta, M.; Eisenangel, S.; Spurlino, J.; Bone, R. Oxyguanidines: application to non-peptidic phenyl-based thrombin inhibitors. *Bioorg. Med. Chem. Lett.* **2003**, *13*, 1495–1498.
- (17) Gandolfi, R.; Gamba, A.; Grünanger, P. 1,3-Dipolar cycloaddition of nitrile oxides to 8-azaheptafulvenes. *Heterocycles* **1995**, *40*, 619–638.
- (18) Malamdou-Xenikaki, E.; Coutouli-Argyropoulou, E. Preparation and catalytic hydrogenation of 1,2,4-oxadiazolo[4,5-*a*]indolines. *Tetrahedron* **1990**, *46*, 7865–7872.
- (19) Kabakov, A. E.; Budagova, K. R.; Maljutina, Y. V.; Latchman, D. S.; Csermely, P. Pharmacological attenuation of apoptosis in re-oxygenated endothelial cells. *Cell. Mol. Life Sci.* **2005**, *61*, 3076–3086.
- (20) Azizian, J.; Madani, M.; Souzangarzadeh, S. One-pot synthesis of novel derivatives of spiro-[6H-indolo[2,1-*b*]quinazoline-6,3'-[1,2,4]oxadiazoline]. *Synth. Commun.* **2005**, *35*, 765–768.
- (21) Tsuge, O.; Kanemasa, S.; Suga, H.; Nakagawa, N. Synthesis of 2-(1-phosphorylalkyl)acetonitrile oxide and its cycloaddition to olefins. Synthetic applications to 3,5-disubstituted 2-isoxazolines. *Bull. Chem. Soc. Jpn.* **1987**, *60*, 2463–2473.
- (22) Selva, M.; Tundo, P.; Marques, C. A. A simple one-pot synthesis of functionalized ketimines from ketones and amine hydrochloride salts. *Synth. Commun.* **1995**, *25*, 369–378.
- (23) Lee, J.-D.; Lee, Y.-J.; Jeong, H.-J.; Lee, J. S.; Lee, C.-H.; Ko, J.; Kang, S. O. Practical synthesis of aminoethyl-*o*-carboranes. *Organometallics* **2003**, *22*, 445–449.

(24) Morimoto, T.; Sekiya, M. A convenient synthetic method for Schiff bases. The trimethyl trifluoromethanesulfonate-catalyzed reaction of *N,N*-bis(trimethylsilyl)amines with aldehydes and ketones. *Chem. Lett.* **1985**, 1371–1372.

(25) Ohtani, I.; Kusumi, T.; Kashman, Y.; Kakisawa, H. High-field FT NMR application of Mosher's method. The absolute configurations of marine terpenoids. *J. Am. Chem. Soc.* **1991**, *113*, 4092–4096.

(26) Reddy, K. L.; Sharpless, K. B. From styrenes to enantiopure *R*-arylglycines in two steps. *J. Am. Chem. Soc.* **1998**, *120*, 1207–1217.

(27) We propose to use the term “druggable motif” to describe some of the well understood pharmacophores that have proven records for achieving good pharmacokinetic, pharmacodynamic, and toxicological profiles. Deliberate attention to suitable “druggable motifs” would help medicinal chemists achieve a balanced approach in evaluating SAR directions. Detailed discussions will be the subject of another publication.

(28) Pozharskii, A. F.; Sitkina, L. M.; Simonov, A. M.; Chegolya, T. N. Nature of the interaction of phenyl and imidazole rings in *N*-aryl-imidazoles. IV. Derivatives of *N*-phenylimidazole with substituents on the benzene ring. *Khim. Geterotsykl. Soedin.* **1970**, *6*, 209–213.

(29) (a) Rubas, W.; Jezyk, N.; Grass, G. M. Comparison of the permeability characteristics of a human colonic epithelial (Caco-2) cell line to colon of rabbit, monkey, and dog intestine and human drug absorption. *Pharm. Res.* **1993**, *10*, 113–118. (b) Makhey, V. D.; Guo, A.; Norris, D. A.; Hu, P.; Yan, J.; Sinko, P. J. Characterization of the regional intestinal kinetics of drug efflux in rat and human intestine and in Caco-2 cells. *Pharm. Res.* **1998**, *15*, 1160–1167.

(30) Ida, N.; Hartmann, T.; Pantel, J.; Schroder, J.; Zerfass, R.; Forstl, H.; Sandbrink, R.; Masters, C. L.; Beyreuther, K. Analysis of heterogeneous A $\beta$ 42 peptide in human cerebrospinal fluid and blood by a newly developed sensitive Western blot assay. *J. Biol. Chem.* **1996**, *271*, 22908–22914.

(31) Lee, J.; Song, L.; Terracina, G.; Bara, T.; Josien, H.; Asberom, T.; Sasikumar, T. K.; Burnett, D. A.; Clader, J.; Parker, E. M.; Zhang, L. Identification of presenilin 1-selective  $\gamma$ -secretase inhibitors with reconstituted  $\gamma$ -secretase complexes. *Biochemistry* **2011**, *50*, 4973–4980.

(32) Wong, G. T.; Manfra, D.; Poulet, F. M.; Zhang, Q.; Josien, H.; Bara, T.; Engstrom, L.; Pinzon-Ortiz, M.; Fine, J. S.; Lee, H.-J. J.; Zhang, L.; Higgins, G. A.; Parker, E. M. Chronic treatment with the  $\gamma$ -secretase inhibitor LY-411,575 inhibits  $\beta$ -amyloid peptide production and alters lymphopoiesis and intestinal cell differentiation. *J. Biol. Chem.* **2004**, *279*, 12876–12882.

#### ■ NOTE ADDED AFTER ASAP PUBLICATION

After this paper was published online December 8, 2011, a correction was made to the straddle heading structure of Table 5. The corrected version was published December 14, 2011.